NASA TECHNICAL MEMORANDUM

NASA TM X-73530

NASA TM X-73530

PERFORMANCE DOCUMENTATION OF THE ENGINEERING MODEL 30 CM DIAMETER THRUSTER

by Robert T. Bechtel and Vincent K. Rawlin
Lewis Research Center
Cleveland, Ohio 44135

TECHNICAL PAPER to be presented at the
Twelfth International Electric Propulsion Conference sponsored by the
American Institute of Aeronautics and Astronautics
Key Biscayne, Florida, November 15-17, 1976

PERFORMANCE DOCUMENTATION OF THE ENGINEERING MODEL 30 CM DIAMETER THRUSTER

Robert T. Bechtel and Vincent K. Rawlin
National Aeronautics and Space Administration
Lewis Research Center
Cleveland, Ohio 44135

E-8952

Abstract

Presented are the results of extensive testing of two 30-cm ion thrusters which are virtually identical to the 900 series Engineering Model Thruster in an ongoing 15 000-hour life test. Included are performance data for the nominal full-power (2650 W) operating point; performance sensitivities to discharge voltage, discharge losses, accelerator voltage, and magnetic baffle current; and several power throttling techniques (maximum I_{sp}, maximum thrust/power ratio, and two cases in between). Criteria for throttling are specified in terms of the screen power supply envelope, thruster operating limits, and control stability. In addition, reduced requirements for successful high voltage recycles are presented.

Introduction

The 30 cm diameter mercury bombardment Engineering Model Thruster (EMT)[1-3] is presently being considered for a variety of planetary and near Earth space missions.[4-6] This variety of missions requires that the thruster be capable of being started, throttled, and operated steady state over a range of input power. This paper describes steady state thruster operation and performance in terms of input power, thrust, specific impulse, control (including high voltage recycle[7,8]), and lifetime over a 4:1 input power range; and dynamic throttling over the same range. (Thruster start-up is detailed in Ref. 7.)

Apparatus

Facility

The tests were conducted in the 3.0-m diameter by 3.0-m long chamber of the 7.6-m diameter by 21.4-m long vacuum tank at NASA's Lewis Research Center. The tank has LN_2 cold walls and was operated at about 5×10^{-6} under load. The thrusters were mounted from the spacecraft simulator frame used in the Multiple Thruster Array program described in Ref. 9.

Power Processors

Laboratory supplies. Most of the steady state performance data were obtained while the thrusters were powered by 12, 60 hertz, laboratory power supplies. The screen and accelerator high-voltage supplies were a high capacity, three phase, full wave bridge rectifier design. The discharge, magnetic baffle, and two keeper supplies were full wave, single phase rectified d.c. sources. The six resistive heaters were powered with alternating current.

Series resonant inverter. All of the control and throttling tests and some performance tests were done with an SCR series resonant inverter power processor unit (ppu) similar to that described in Ref. 10. This ppu has 12 flight type power supplies. While the specific design, such as output impedance, of the resistive load supplies does not significantly effect thruster control or operation, this is not necessarily true of the plasma load supplies. Therefore, pertinent characteristics of these five supplies are given in Table I.

Fifteen analog voltage set points were available for each of the discharge current, beam current reference, screen voltage, and magnetic baffle operating parameters. These were selected to provide 15 distinct input power levels. Throttling was performed by external logic which sequentially switched each of the four set points. The discharge current, beam current reference, and screen voltage were simultaneously switched directly to their new values. The magnetic baffle current was first switched to zero and then to its new value.

Thrusters

Two engineering model 30 cm diameter thrusters, designated S/N 802 and 804, were used for this investigation. These thrusters were equivalent to the 900 series thruster of Ref. 11 in all areas affecting thruster performance and thruster-ppu interface requirements. These modified 800 series and the 900 series thrusters evolved from the 700 series design which was life tested in 1974[2] for 10 000 hours. Vibration tests of the 700 series thruster necessitated some structural changes leading to the 800 series design.[12] The life test of Ref. 2 defined several wear out modes which required modifications. These modifications were determined by a series of tests performed at Lewis Research Center and detailed in Ref. 3.

Other changes included the change of the cathode insert design from a rolled tantalum foil type to an impregnated type to provide better neutralizer closed loop control and overall component quality control. The heater type was changed from the flame-sprayed design to a swaged construction.[13]

These were the major modifications to the 700 and 800 series thruster design of Ref. 12 which resulted in the current engineering model (900 series) thruster design.

Results and Discussion

Four basic parameters are normally used to evaluate thruster performance. These are the output performance parameters of (1) thrust, T; (2) specific impulse, I_{sp}; (3) total efficiency, η_T; and the input performance parameter of total input power, P. The equations, assumptions, and approximations used to derive these thruster performance parameters are detailed in the appendix. The only thruster operating parameters which appear in the performance calculations (see appendix) were beam current, J_B; screen voltage, V_I; discharge chamber losses, ε_T; and total propellant flow rate, $\dot{m}_0$. The first three parameters can be selected and held by the power processor. The mass flow rate, however, is a function of several other operating

STAR category 20

parameters; specifically, discharge voltage, ΔV_I; accelerator voltage, V_A; discharge losses, ϵ_I; and cathode tip power (and temperature), P_{CT}, and magnetic baffle current, J_{mB}. Tests were conducted to determine the variations of performance parameters with changes in operating parameters to define the operating points over a 4 to 1 range of input power, consisting with thruster lifetime and control, followed by an implementation of several throttling profiles and schemes.

Thruster Performance - Steady State

Cathode tip power. Thruster testing of an impregnated insert recessed 6.3 mm from the cathode tip showed poorer performance compared to tests with a rolled foil insert. Because of the difference in the thermal characteristics of the two insert types, tests were conducted to determine the effects of cathode temperature on thruster performance. Fig. 1 shows the effect of cathode tip power on propellant flow rate at a given operating point. Addition of tip heater power did not significantly affect cathode flow rate, but did reduce the main flow rate with a corresponding increase in utilization efficiency. This improvement in performance was due to improved emission characteristics resulting in a reduced cathode sheath voltage drop as characterized by decreases of several volts in the cathode keeper voltage. As discussed in Ref. 14, such a sheath voltage decrease results in a net increase in electron energy and a subsequent increase in the ion production rate in the discharge, and, hence, improved performance.

Rather than operate with the heater supply constantly on to maintain sufficient cathode insert temperature, the insert was moved forward, flush with the cathode. This resulted in increased operating temperatures as shown in Ref. 14. The performance of thrusters SN 802 and 804 with this insert position is shown in Fig. 2. The main propellant flow rates are virtually the same for both thrusters when operated at the same cathode flow rate.

Some slight variations in thruster performance were noted when cathode tip heater power was applied with a flush insert. However, this mode of operation was undesirable because of the additional power requirements and complexity and as a result was not investigated.

Discharge voltage and losses. - Two operating parameters which directly effect the mass flow rate and therefore the thruster output parameters are the discharge voltage, ΔV_I, and the discharge losses, ϵ_I. This section details the criteria for the selection of these two parameters and examines the trade between discharge power requirements and propellant mass flow rate.

Table II shows the variation of flow rate and total efficiency for changes in ΔV_I and ϵ_I at a screen voltage of 1100 volts and beam currents of 1 and 2 amps. The total efficiency was calculated using the thrust correction factors as discussed in the appendix.

Based on the lifetime projections of Ref. 3, the maximum discharge voltage considered for a 2 A beam was 36 V. A reduction of the discharge voltage would further increase expected lifetimes. But, as shown in Table II, a 1 V decrease would also cause a total efficiency decrease of 0.015. This is the most sensitive total efficiency variation shown in Table II. At the 1 A operating point, the sensitivity is 2.5 times less.

The discharge voltage was selected as 36 V over the operating range based on the following considerations:

(1) Significant total efficiency penalties of as much as 0.015 percentage points/V below 36 V at 2 A beam

(2) Expected lifetime penalties due to sputter erosion at discharge voltages in excess of 36 V at 2 A beam

(3) An overall simplification of the control philosophy when using a single discharge voltage set point over the operating range

(4) A lack of performance sensitivity to discharge voltage at the 1 A beam current level

As the discharge losses are increased at constant discharge voltage, and beam current, the utilization efficiency increases as the power efficiency decreases. Since the total efficiency is proportional to the product of the utilization and power efficiencies (consistent with the assumptions detailed in the appendix), there is a trade between these two efficiencies by which the total efficiency can be maximized. Operation near this maximum total efficiency is one consideration in the selection of the discharge loss operating point.

There are other factors which affect maximum and minimum discharge loss operating points. For example, a practical maximum at a 2 A beam current can be expressed in terms of a maximum emission current consistent with demonstrated cathode lifetimes. Another consideration must be a trade of power supply capability and weight or design. These factors have resulted in a selection of 198 eV/ion as a 2 A beam maximum discharge loss operating point. Table II shows increases above 198 eV/ion to 211 eV/ion (6.5%) to increase total efficiency by less than 0.005. Similar increases at a 1 A beam current shows an increase in total efficiency of less than 0.001.

The minimum discharge losses are governed primarily by the ability to maintain closed loop control of the discharge. Fig. 3 illustrates a condition commonly referred to as "low mode." As the discharge losses are decreased, the main flow rate is increased to maintain a constant beam current, and the propellant utilization efficiency decreases as evidenced by the increasing impingement current in Fig. 3. Eventually a point is reached where the beam current actually begins to decrease with increasing flow, resulting in a runaway condition of the main flow rate control loop and rapidly increasing impingement currents. This occurs at ~180 eV/ion for a 2 A beam current in Fig. 3. The value of this minimum eV/ion was about the same over the throttle range.

The definition of "minimum eV/ion" is arbitrary, but the operating point must be selected to provide ample margin so that minor perturbations, drifting, or aging cannot cause the thruster to go into low mode. Selection of the 198 eV/ion operat-

ing point provides a margin of about 10%.

The data of Table II show a significant decrease in the total efficiency gain/(eV/ion) in going from 198 to 215 eV/ion as opposed to going from 185 to 198 eV/ion. This suggests that the 198 eV/ion operating point (at 1 A beam) is near the point of maximum total efficiency as discussed previously. Further increases in discharge losses would be expected to decrease the power efficiency faster than increasing the utilization efficiency, thereby resulting in a decrease in the total efficiency.

There does not appear to be a significant reason for increasing the discharge losses at reduced power operation. In fact, simplicity of control again presents a strong argument for throttling at constant discharge losses of 198 eV/ion.

Accelerator voltage. - The primary purpose of accelerator voltage is to prevent electron backstreaming. However, several other factors concerning accelerator voltage have been observed to affect thruster operation before backstreaming becomes an effect.

Reducing the accelerator voltage forces operation nearer the perveance limit of the extraction system. This limit is defined as that accelerator grid system voltage/current operating point where the ion focusing is barely adequate to prevent direct ion impingement and is shown in Fig. 4. Moving the operating point nearer the perveance limit affects total efficiency, accelerator grid lifetime, and increases ion defocusing resulting in increased sputtering of downstream components.

Table II shows a slight effect of accelerator voltage on total efficiency. Decreasing the accelerator voltage from 500 to 300 V causes decreases in total efficiency of ≤ 0.003 at 2 and 1 A beam currents. This decrease is due entirely to a decrease in the propellant utilization efficiency.

There are several reasons for considering reducing of the accelerator voltage and accepting the decrease in performance. Ref. 15 shows better focusing of ions from a typical aperture near the center portion of the grid. Lack of focusing (or angular dispersion) is one possible cause of the chamfering of the upstream edges of the accelerator apertures as noted in the 10 000 hr test of Ref. 2.

Another reason involves ions which leave the peripheral grid apertures at angles as great as 80°. Reducing the accelerator voltage also serves to reduce the number of these ions.[15] High angle ions are the most probable cause of ground screen and neutralizer erosion noted in the life test.[2]

An additional consideration is the erosion of the accelerator grid due to charge exchange ions. The measured charge exchange erosion rate on the 10 000 hr grid of Ref. 2 indicated a potential problem if grid lifetimes of 15 000 hrs are desired. Reduction of the accelerator voltage from 500 to 300 V could reduce the sputtering rate of the grid by as much as a factor of 2.

Magnetic baffle. - The magnetic baffle current strongly affects the operating character of the thruster. Variation of the magnetic field within the discharge chamber via the magnetic baffle current affects the performance and controlability over the throttling range. Improper set point can cause discharge instabilities and attendant control problems, excessive cathode propellant flow rate and attendant sputter erosion of discharge components, or change in the character of the discharge oscillations. The tests described were designed to establish the criteria for selection of the magnetic baffle current set point over the throttling range.

The basic result of a change in the magnetic baffle current is a shift in the discharge voltage-ampere characteristic in much the same way as a change in the cathode propellant flow rate shifts this characteristic. Thus the magnetic baffle current is a means to set the cathode flow rate, which, as seen in Fig. 2, is the parameter which must be specified when defining or comparing thruster operation and performance.

Fig. 5 shows the variation of discharge voltage with cathode flow rate for several magnetic baffle currents. These curves were generated by slowly varying the cathode vaporizer temperature open loop and recording the cathode vaporizer temperature-discharge voltage. Subsequently, the cathode flow rate was measured at a discharge voltage of 36 V.

The discharge operation of Fig. 5 can be divided in four regions at a discharge voltage of 36 V:

(1) Low flow region, $\dot{m}_c < 80$ mA

(2) Normal operation region, 80 mA $< \dot{m}_c <$ 100 mA

(3) Bistable operation region, 100 mA $< \dot{m}_c <$ 120 mA

(4) High flow region, 120 mA $< \dot{m}_c$

In the low flow region, the flow rate/discharge voltage control characteristic is monostable, but the gain is sufficiently high to cause control limit cycling and hunting under some circumstances. These considerations are discussed in Ref. 16. Fig. 6(a) shows oscilloscope traces for low flow operation. Note the large amplitude, low frequency random type spikes on the discharge current and voltage traces. This is accompanied by large current spikes on the cathode vaporizer current as the controller tries to track the discharge voltage.

The normal operation region is shown in Fig. 6(b). Discharge voltage and current and beam current are periodic and free of large amplitude spikes. The control characteristic slope of Fig. 5 is reduced from the low flow region and stable control of the discharge voltage is readily achieved.

The bistable region has two operating points, occurring at the intersection of the desired set point (36 V) and the negative slopes of the curves of Fig. 5. Any minor perturbation can cause a switch from one operating point to another.

High flow operation is shown in Fig. 6(c). There are no large current or voltage spikes, but the oscillations are random and incoherent. Moreover, to be able to operate above the double valued

portion would require cathode flow rates of 0.130 A (eq) or more.

Low flow operation is not desirable for several reasons. Large current and voltage spikes can adversely effect projected lifetime, since wear mechanisms are nonlinear with current and voltage. These spikes also make it more difficult for the cathode vaporizer control loops to maintain a constant d.c. discharge voltage level. Further, these variations are potentially sources of conducted and radiated noise since they do involve rapid switching of relatively large currents and voltages. The noise problems associated with the low flow region are unknown and difficult to assess, but they would probably impose significant filtering burdens on the power processor. As a result, the onset of discharge chamber oscillations as shown in Fig. 6(a) represents a practical minimum acceptable magnetic baffle operating current.

Bistable operation is undesirable because of the uncertainty in the magnitude of the cathode flow rate at the controlled discharge voltage and the associated control problems. High cathode flow region is undesirable from a lifetime viewpoint. Ref. 3 indicates internal discharge chamber erosion to be a significant function of cathode flow rate. Erosion rates increased by a factor of about 1.5 when the cathode flow rate increased from 80 to 120 eq mA. Thus, the region which appears best suited for a steady state set point is the normal operation region.

Fig. 7 shows the effect of magnetic baffle current on thruster performance at a discharge voltage of 36 V and discharge losses of 198 eV/ion. As the magnetic baffle current is increased through normal operation, the cathode flow rate increases and the main flow rate decreases, such that the total flow rate remained nearly constant. As a result, the propellant utilization efficiency throughout the normal operation region varies less than 0.006. In fact, the total variation over all four regions is only 0.008.

Based on the conclusions from Figs. 5 through 7, it is apparent that specifying the limits of the normal operation region is sufficient for specifying the magnetic baffle current since (1) this region is preferred for control and lifetime considerations and (2) the thruster performance is relatively insensitive to variations in magnetic baffle current, especially in the normal operation region.

Screen voltage and current. The proposed mission set presents several general requirements for the 30 cm thruster operating point. These are (1) specific impulse of ~3000 sec at full power, (2) a maximum input power of 2650 W, and (3) the capability of throttling over an input power range of 4:1.

The first two points require maximum operating limits for the screen voltage and current of 1100 V and 2 A, respectively, thus specifying the power supply envelope. Operation at 1/4 power eliminates from consideration any screen voltage/current steady state operating point resulting in power less than 662 W. The beam current capability of the extraction system determines the minimum screen voltage. Operation below 600 V is generally unattractive for any beam current in excess of 0.5 A and this minimum screen voltage increases with increasing beam current in order to maintain adequate grid perveance (Fig. 4). Steady state operation at any screen voltage/current set points within these limitations is acceptable for achieving a 4:1 input power throttle range. It is, however, necessary to evaluate the effect of the screen voltage/current set points within this operating envelope on the thruster performance parameters.

Fig. 8 shows the V_I vs J_B map of permissible operating points. The lines of constant power were calculated using a fixed discharge loss of 198 eV/ion and fixed power losses of 50 W. The minimum perveance limit is determined by including the V_{TOT} vs J_B relationship shown in Fig. 4 and assuming an accelerator voltage of 300 V. Thus

$$V_I = V_{TOT} - 300 = f(J_B) - 300$$

If the accelerator voltage is increased, the screen voltage can be decreased by approximately an equal increment. The perveance limit in the Fig. 8 provides no margin, and in actual practice operation on this line probably would cause some stability and control problems.

The thrust is also a function of V_I and J_B only, permitting lines of constant thrust/power ratio to be included in Fig. 8. However, the specific impulse and total efficiency are also functions of mass flow rate. This additional information must be considered in evaluating a particular operating point within the envelope of Fig. 8.

The measured propellant utilization efficiency, specific impulse, and total efficiency at various input power levels are shown in Fig. 8 and Table III. Note that the propellant utilization efficiency is not a strong function of the voltage/current trade above 1/2 input power. Below 1/2 power the measured utilization efficiency decreases more significantly with decreasing beam current.

The specific impulse at constant power is seen to vary monotonically with increasing voltage and decreasing current. Even at 1/4 power, the effect of a 500 V change in screen voltage has a greater effect on the specific impulse than the measured change in utilization efficiency. Similarly, the increase in propellant utilization efficiency realized by increasing the current and decreasing the voltage is never great enough to offset the decrease in power efficiency. As a result, the maximum efficiency always occurs at the maximum screen voltage of 1100 V.

There are, however, other factors to be considered in selecting a set point, especially at the lower input power levels where control can be a major concern.

Fig. 9 shows oscilloscope traces of discharge voltage and current at 1/4 power operating points. The two operating points shown (1100 V, 0.47 A; 605 V, 0.76 A) are the two limiting cases of the voltage/current trade-off determined by the power supply operating envelope (Fig. 8). The oscillations at 0.47 A beam are nonperiodic and random with peak to peak current variations of ~4 A about a d.c. level of 3.05 A.

The voltage shows some peaks which approach 20 V above the 36 V d.c. level. However, the oscillations at the 0.76 A point are smaller in magnitude with a definite frequency of ~3 kHz. Further, strip chart recordings of the two vaporizer currents show significant increases in the noise components of these currents for the 0.47 A beam. This is due to the control loops attempt to control the spikes seen in Fig. 9.

Another reason for considering the 600 V, 0.76 A point for 1/4 power is the thermal data of Table IV (see also Ref. 14). Although no problems have been experienced due to a cool feed system, the 10% higher isolator flange temperatures are an advantage since they reduce the probability of requiring isolator heater power in any thermal environment.

The same argument also applies to the probability of requiring cathode tip heater power since the higher discharge power and current significantly increases the cathode self-heating.[14]

Although, as will be seen, throttling at maximum screen voltage is possible, a qualitative assessment of thruster operation suggests that strong preference be given to throttling by reducing the screen voltage as well as the beam current, at least at levels below 1/2 power.

Vaporizers, heater, keeper supplies. - The selection of the operating parameters of the remaining eight supplies do not significantly affect the thruster performance parameters, but a brief description of these supplies is presented here.

The three vaporizer supplies are normally in closed loop proportional control, and as such have their set points controlled by operating parameters of other supplies.

The three heater supplies, cathode tip, neutralizer tip, and isolator are currently used only for start up and normally have zero output during steady state operation.

The cathode keeper supply aids discharge stability at low discharge current and during recycle. This supply is operated at 1 A with the voltage uncontrolled. The power consumed ranges from 5 to 9 W typical over the throttling range due to variation of keeper voltage with beam current set point.

The neutralizer keeper was operated at 1.8 A for all beam current levels. Although the neutralizer keeper voltage vs. mass flow characteristic was not mapped for these tests, other tests have indicated that a keeper voltage of 15 V results in mass flow rates of ~30 equivalent mA at a 2 A beam. As the beam current is reduced, the neutralizer keeper voltage set point generally has been increased to about 17.0 V to maintain stability and low neutralizer flow rate. These neutralizer operating conditions were assumed for calculations made in this paper.

Dynamic Throttling

The previous sections have defined the criteria for selection of all thruster steady state operating parameters. This section investigates the dynamic sequencing of set points over several throttling profiles covering a 4:1 input power range.

Four throttling profiles were selected for testing. These are shown in Fig. 10. Profile 1 maintains a constant screen voltage of 1100 V over the 4:1 input power range. This maximizes both total efficiency and specific impulse. Profile 2 was identical to profile 1 down to a beam current of 0.9 A. However, due to the preference of reducing screen voltage rather than beam current to attain steady state operation at 1/4 power, profile 2 was selected to reduce both voltage and current below 0.9 A as shown in Fig. 10. Profile 3 was selected as a compromise profile in which the beam current was decreased from 2.0 to 0.76 A proportional to the decrease in input power from 2650 to 662 W. The selection of current and power fixed the screen voltage as shown in Fig. 10. Profile 4 was an attempt to throttle as close to the perveance limit as practical. This profile represents a maximum thrust/power ratio at any given thruster input power. The minimum screen voltage at a given beam current as shown by profile 4 of Fig. 10 was determined by the stability of the proportional control loops and not by a thruster operating limitation. Improved control stability[16] should permit operation closer to the true thruster limit represented by the perveance limit shown in Fig. 10.

Once the screen voltage and beam current had been specified, it was necessary only to specify the magnetic baffle current for each operating point. The criterion used was to maintain operation within the normal operating range as discussed previously. Variation of the magnetic baffle current at various operating points resulted in the maximum-minimum limits for each of the four profiles. These normal operating envelopes are shown in Fig. 11.

The effect of decreasing the screen voltage at a given beam current is to shift the entire normal operating envelope to the higher magnetic baffle currents. This is especially evident when comparing profiles 1 and 2 to profile 3. The difference between profiles 3 and 4 was found to be very slight. Also note the narrow, double-valued portion of the profile 1 envelope below 0.7 A beam current. The uncertainties associated with control in this region re-enforces the preference for a throttling profile which reduces the screen voltage while maintaining higher beam currents.

With the definition of the operating envelopes, an arbitrary magnetic baffle current was selected near mid-range over throttling profile 1. The first attempt to throttle up from 0.9 to 2.0 A beam revealed no problems. However, when the throttle direction was reversed, difficulties were experienced. Fig. 12 shows strip chart recordings of the critical thruster operating parameters during the throttle down mode. At beam currents below 1.6 A, there appears a large increase in discharge voltage during the first cycle of the cathode vaporizer controller. This results directly in a noisy beam current condition.

In order to analyze this operation, it must be remembered that the initial change in electrical operating parameters is done at effectively constant flow rate. Thus when the emission current is decreased, the discharge voltage decreases. The

proportional controller begins to decrease the cathode propellant flow rate. However, if the magnetic baffle current, cathode flow rate operating point is too near the minimum boundary of the operating envelope, the actual set point will momentarily move out of the envelope and into the low cathode flow operation, although eventually the control loops will settle within the normal operation limits. This is not observed when throttling up since the argument is reversed, although transient operation in the high flow region may occur.

The impact of even momentary operation in the low cathode flow region is difficult to assess. There is, however, potentially a significant effect on power processor and/or spacecraft noise susceptibility and filtering constraints.

Although it is possible that a control loop modification could reduce this problem, the most direct solution was found to be raising the magnetic baffle current set point in the problem area of the throttling profile. By increasing the magnetic baffle current set point by as much as 0.3 A in the region from 1.6 to 0.9 A beam current, this problem was eliminated.

An iterative process of selecting magnetic baffle currents within the normal operating envelope of Fig. 12 was carried out for each operating set point along all four profiles. The set points defining each of these profiles is given in Table V. The dynamic throttling results are illustrated in the strip chart recordings of Fig. 13. Each of these profiles were repeated for time increments of 6.3, 22.5, and 38.9 sec in addition to the increment of 14.4 sec, shown. No effect was noted for this variation.

Thruster Performance - Throttling

Fig. 10 has shown the variations of thruster performance parameters throughout the operating envelope. The previous section has demonstrated four profiles over which the thruster operating parameters can successfully be sequenced to achieve a 4:1 change in input power. Fig. 14 and Table VI show the variation of the performance parameters as the thruster operating parameters are sequenced over each of the four profiles.

As noted before, profile 1 shows the highest total efficiency and specific impulse over the throttling range. Profile 2, however, does not suffer a large efficiency penalty at the low throttle points as does profile 1. At 1/4 power the difference in total efficiency is less than 0.01. There is a specific impulse penalty realized over the lower 1/3 of the throttling profile, amounting to ~19% at 1/4 power. This specific impulse penalty may mean increased propellant weight, but can be traded against a 19% increase in the thrust/power ratio. The significant advantage of profile 2 is much better control as compared to profile 1.

Profile 3 does provide a good all around compromise. Efficiency penalties are less than a percent and the thrust to power ratio is significantly increased over profiles 1 and 2 over the lower 2/3 of the throttling range. Further, acceptable control was realized over this throttling profile. In general, profiles 2 and 3 appeared to provide the best throttling control, the former at high efficiency and specific impulse, the latter at high thrust to power ratio.

Profile 4 is of interest only where thrust is to be maximized for a given power input, since this profile corresponds to minimum efficiency and specific impulse over the throttling range. Efficiency penalties can be as much as 2% or more near the 1/2 power point. An additional disadvantage of this profile is the difficulty of control.

High Voltage Recycle

The high voltage recycle profile of the power processor used in these tests qualitatively is the same as the profile described in Ref. 7. The differences in these recycle profiles will be discussed later. Fig. 15 shows a typical recycle for a 2 A beam current. When the overcurrent condition is sensed by the power processor logic, the high voltage supply is turned off, the discharge current reduced, and the neutralizer keeper current (not shown in Fig. 15) increased. After 150 msec, the high voltage is commanded on, and 20 msec after that, the discharge and neutralizer keeper currents are commanded back to their run levels. The total recycle sequence is complete in less than 300 msec. Since this is much faster than the thermal response of the propellant feed systems, there is no need for changes in the vaporizer control loops or heater set points.

The recycle sequence described was verified over the four throttling profiles of Fig. 10. This was done by momentarily shorting the accelerator supply, causing electron backstreaming from the neutralizer to initiate the overcurrent command and begin the recycle sequence. The current in the shorting path was sensed to trigger the first oscilloscope which in turn triggered the second scope.

Figs. 15 to 17 show the recycle sequence for the end points of the four throttling profiles of Fig. 10. In addition 2 intermediate points (not shown) were verified for each of the four throttling profiles.

Although the present recycle and the recycle of Ref. 7 are qualitatively the same, there are some significant quantitative differences which are a result of the specific control logic and power supply designs and limitations. The most significant power supply difference is in the high voltage supplies. These two supplies in the present power processor are inherently current limited. Thus transient arcs at the thruster tend to become self-extinguishing as the supply voltages load down. This is seen in Fig. 15(b). Approximately 2 msec after the supply is turned on, a beam current transient occurs, loading down the high voltage supplies until the transient can no longer be sustained. In the case of noncurrent limited supplies, as in Ref. 7, the supply will try to maintain a constant voltage, thereby sustaining the current transient until external overcurrent protection circuitry generates the appropriate supply off commands.

Another significant difference is the discharge supply output impedance. With an output, choke in the present supply, discharge current oscillations are significantly reduced. This permitted the higher discharge current cut back levels without problems of the discharge extinguishing.

Finally control logic differences provide for better high voltage regulation, control of timed intervals, and slower rate of increase of the discharge current. The combination of these changes has resulted in a reduction of the high voltage off time and discharge current cut back times below the limits suggested in Ref. 7.

The profiles of Figs. 15 through 17 work satisfactorily at any point within the screen supply/thruster operating envelope and thus recycle is not a factor in the selection of a throttling profile. Further, it does appear that the success of a short (≤1 sec) recycle is primarily a function of the power supply dynamics at all of these operating points.

Conclusion

Three specific areas of thruster operation have been considered: (1) variation of thruster performance parameters with thruster operating parameters, (2) modes of throttling over a 4 to 1 range of input power, and (3) high voltage recycle at various operating points over the throttle envelope. These areas have been investigated from the standpoint of thruster performance, control, and interface with power processor.

The changes in thruster performance parameters, input power, thrust to power ratio, specific impulse, and total efficiency were determined in terms of changes in thruster operating parameters.

Increasing the recessed cathode insert temperature by the addition of cathode tip heater power increased the propellant utilization efficiency by several percent. Repositioning the impregnated insert flush with the cathode face sufficiently increased the insert temperature to result in similar performance gains without the addition of heater power.

Within the range of operating parameters investigated, the discharge voltage had the most pronounced effect on total efficiency: as much as 1.5% increase per volt increase. The discharge losses and accelerator voltage were found to have less of an effect on the performance parameters. The magnetic baffle current was found to have an effect on discharge oscillations and control more than on performance parameters, the total mass flow rate being somewhat independent of magnetic baffle current for a fixed set of operating parameters. Thus the magnetic baffle current could be selected based on operational stability rather than performance. The discharge operating parameters were specified as 36 V and 198 eV/ion (emission current/beam current = 6.5) for the throttle envelope.

Variation of the screen voltage and beam current at constant input power showed that the specific impulse varied monotonically with screen voltage, since the mass flow rate varied almost linearly with beam current.

The increase in propellant utilization efficiency as the beam current was increased at constant power, was more than offset by the decrease in power efficiency resulting from the more pronounced effect of discharge energy losses when compared with screen voltage. Thus the maximum total efficiency was also consistent with maximum screen voltage. The maximum variation in specific impulse at constant power between maximum and minimum screen voltage was about 500 sec while the maximum variation in total efficiency was about 5 percentage points. Both maximum variations occurred slightly below the 1/2 power point. The maximum thrust to power ratio was found to occur, as expected, at the lowest screen voltage for a constant input power.

Four throttling profiles were tested. One maintained maximum total efficiency and specific impulse, and a second maintained maximum thrust to power ratio. However, each of these two did present undesirable control characteristics. As a result, two compromise profiles were also defined between the two extremes. Throttling along each of these profiles could be achieved in 15 steps in time increments as small as 6 sec/step.

Finally effective high voltage recycle was demonstrated throughout the throttling envelope. The recycle sequence lasted less than 300 msec, and as a result, no vaporizer or other thermal input variations were required during recycle. Only the high voltages, discharge current, and neutralizer keeper current were affected. Differences in the character of the present recycle and previous sequences were found to be more a function of power supply control logic and dynamics rather than thruster operating characteristics.

Total efficiencies ranged from 0.70 at an input power of 2650 W to 0.466 at an input power of 662 W.

Appendix

Thruster Performance Calculations

The ideal thrust of an ion thruster using mercury propellant can be expressed in terms of the electrical operating parameters as

$$T_{IDEAL} = 2.0391\ J_B\sqrt{V_I}\ \text{mNt} \qquad (1)$$

where the units of J_B and V_I are amperes and volts and defined in Fig. A1. In this ideal case the ions are assumed to be only singly charged and axial in direction.

In reality the ion beam of the 30 cm EMT contains a nonnegligible number of doubly charged ions as well as ions of both species which are not axial in direction.

A technique for evaluating the thrust losses due to these doubly charged ions and nonaxial ion trajectories, using a collimating mass spectrometer and computer program has been developed by Hughes Research Labs under NASA contract.[15,17] This measurement yields two thrust correction factors; α, which accounts for the different ion charge to mass ratios, and F_t, which accounts for nonaxial trajectories. The product of these two factors and the ideal thrust calculated from metered parameters give the actual thrust.

$$T_{ACT} = \alpha F_T\ 2.0391\ J_B\sqrt{V_I}\ \text{mNt} \qquad (2)$$

A detailed map of these two parameters is given in Ref. 15. Although a variety of thruster parameters affected both α and F_t, to a first approximation, they can be considered to vary only with beam

current.

All of the data presented for a given beam current in Ref. 15 are within 0.9% of the average value for that beam current. Fig. A2 shows the average value of (αF_t) as a function of beam current. The values of this parameter are taken from Fig. A2 for all calculations made in this paper.

The total power input to the thruster is given by summing the product of voltage and current of each of the twelve power supplies. (See Fig. A1 for location of measurements and definitions.) Thus

$$P_T = (V_S)J_S + \Delta V_I J_I + V_A J_A + P_{VAP} + P_{HTR} + P_{CK} + P_{NK} + P_{MB} \quad (3)$$

The first three terms are the power in the screen, discharge, and accelerator supplies. These voltage and currents must be selected to provide the best overall performance. The term P_{VAP} is the total power to the three vaporizers; the term P_{HTRS} the total power to the cathode, neutralizer, and isolator heaters; and P_{CK} and P_{NK} are the cathode and neutralizer keeper powers, respectively. Although the magnetic baffle current significantly affects thruster operation, the power dissipated is small. The accelerator power is also small being typically less than 2 W over the throttle range. A summary of each of these powers is given in Table AI for typical operation at beam currents of 2.0 and 0.5 A. The last six terms of Eq. (3) are assumed to equal 50 W and be independent of thruster beam current or input power.

Using the relations

$$J_S = J_B + J_A = J_B$$

$$J_I = J_E + J_B$$

$$\epsilon_I = \Delta V_I \, J_E/J_B$$

$$V_S = V_I - \Delta V_I + |V_G| = V_I$$

Eq. (3) becomes

$$P_T = (V_I + \epsilon_I)J_B + 50 \text{ W} \quad (4)$$

The actual thrust to power ratio can then be expressed from Eqs. (2) and (4) as

$$\frac{T}{P} = \frac{\alpha F_t \; 2.0391 \; J_B\sqrt{V_I}}{J_B(V_I + \epsilon_I) + 50} \; \frac{mNt}{W} \quad (5)$$

Total thruster efficiency is defined as

$$\eta_T = \frac{T^2}{2\dot{m}_o P_T} \quad (6)$$

Substituting Eqs. (2) and (4) into Eq. (6) yields

$$\eta_T = \frac{(\alpha F_T)^2 \, JB^2 \, V_I}{\dot{m}_o[J_B(V_I + \epsilon_I) + 50]} \quad (7)$$

where $\dot{m}_o$ is the neutral mass flow rate expressed in equivalent amperes.

Eq. (7) can be expressed in terms of the measured propellant utilization efficiency as

$$\eta_T = \alpha F_T^2 \eta_u \times \eta_p$$

where both η_u and η_p are directly measured values which are uncorrected for any double ionization.

The specific impulse, defined as the total impulse divided by the propellant weight can be expressed as

$$I_{sp} = 100.08 \; \alpha F_T \frac{I_B}{\dot{m}_o} \sqrt{V_I} \text{ sec} \quad (8)$$

References

1. Sovey, J. S., and King, H. J., "Status of 30 cm Mercury Ion Thruster Development," AIAA Paper 74-1117, Oct. 1974.

2. Collett, C. R., "Thruster Endurance Test," Hughes Research Labs, Malibu, Calif., NASA CR-135011, May 1976.

3. Manitenieks, M. A., and Rawlin, V. K., "Studies of Internal Sputtering in a 30-cm Ion Thruster," AIAA paper 75-400, Mar. 1975.

4. Duxbury, J. H., "An Integrated Solar Electric Spacecraft for the Encke Slow Flyby Mission," AIAA Paper 73-1126, Oct.-Nov. 1973.

5. Gilbert, J. and Guttman, C. H., "Evolution of the SEP Stage/SEPS/Concept," AIAA Paper 73-1122, Oct.-Nov. 1973.

6. Masek, T. D., Richardson, E. H., and Watkins, C. L., "Solar Electric Propulsion Stage Design," AIAA Paper 73-1124, Oct.-Nov. 1973.

7. Bechtel, R. T., "Control Logic for a 30 cm Diameter Ion Thruster," AIAA Paper 75-378, Mar. 1975.

8. Terdan, F. F., and Bechtel, R. T., "Control of a 30-cm Diameter Mercury Bombardment Thruster," AIAA Paper 73-1079, Oct.-Nov. 1973.

9. Rawlin, V. K., and Mantenieks, M. A., "A Multiple Thruster Array for 30-cm Thrusters," AIAA Paper 75-402, Mar. 1975.

10. Beiss, J. J., and Inouye, L. Y., "Power Processor for a 30 cm Ion Thruster," TRW Systems Group, Redondo Beach, Calif., TRW-20384-6002-RU-01 (NASA CR-134785), Oct. 1974.

11. Collett, C. R., and Bechtel, R. T., "Endurance Test of a 900 Series 30-cm Engineering Model Ion Thruster," Proposed AIAA paper 76-1020, Key Biscayne, Fal., 1976.

12. Schnelker, D. E., and Collett, C. R., "30 cm Engineering Model Thruster Design and Qualification Tests," AIAA Paper 75-341, Mar. 1975.

13. Mueller, L., "High Reliability Cathode Heaters for Ion Thrusters," AIAA Paper 76-1071, Key Biscayne, Fla., 1976.

14. Mirtich, M. J., and Kerslake, W. R., "Long Lifetime Hollow Cathodes for 30 cm Mercury Ion Thrusters," Proposed AIAA Paper 76-985, Key Biscayne, Fla., 1976.

15. Poeschel, R. L., et al., "A 2.5 kW Advanced Technology Ion Thruster," Hughes Research Labs., Malibu, Calif., 1976, CR-135076, NASA 1976.

16. Robson, R. R., "Compensated Control Loops for a 30 cm Ion Thruster," Proposed AIAA paper 76-994, Key Biscayne, Fla., 1976.

17. Poeschel, R. L., "A 2.5 kW Advanced Technology Ion Thruster," Hughes Research Labs, Malibu, Calif., NASA CR-134687, Aug. 1974.

Table I Characteristics of series resonant inverter plasma load power supplies

Supply	Maximum ratings	Last stage output filter	Comments
Screen	1100 V, 2.1 A	2 μfd parallel	Overcurrent protection at 2.1 A; overcurrent condition generates high voltage recycle command
Discharge	45 V, 14 A	0.5 mhy series	
Accelerator	515 V, 0.1 A	0.1 μfd parallel	Common transformer with screen supply - turns ratio yields accel voltage of 0.47 times screen voltage
Neutralizer keeper	25 V, 3 A	3 mhy series	
Cathode keeper	25 V, 1 A	0.01 μfd parallel	

Table II Summary of performance variations for changes in operating parameters

[V_I = 1100 V]

ΔV_I, v	ε_I, eV/ion	V_A, v	J_B, A	$\dot{m}_m$, eq. mA	$\dot{m}_c$, eq. mA	$\dot{m}_o$, eq. mA (a)	η_u	P_T, W	η_p	η_T	Total efficiency variation
36	210	500	2	2018	78	2126	0.941	2670	0.824	0.7012	0.015 V
35	210	500	2	2050	92	2172	.921	2670	.824	.6860	
37	198	300	1	1099	112	1241	0.806	1350	0.815	0.6168	0.006/V
35	198	300	1	1127	109	1266	.790	1350	.815	.6046	
36	198	500	2	2047	82	2159	0.926	2646	0.831	0.6959	0.0045/13 eV/ion
36	211	500	2	2018	78	2126	.941	2670	.823	.7004	
36	185	300	2	2093	78	2201	0.909	2620	0.840	0.6906	0.0008/13 eV/ion
36	198	300	2	2071	74	2175	.920	2646	.831	.6914	
36	185	300	1	1146	115	1291	0.775	1335	0.824	0.5996	0.0103/13 eV/ion
36	198	300	1	1119	108	1257	.796	1348	.816	.6099	.0008/17 eV/ion
36	215	300	1	1098	111	1239	.807	1365	.806	.6107	
36	198	300	2	2071	74	2175	0.920	2646	0.831	0.6914	0.002/100 V
36	198	500	2	2047	82	2159	.926	2646	.831	.6959	
36	198	300	1	1119	108	1257	0.796	1348	0.816	0.6099	0.003/100 V
36	198	500	1	1095	117	1242	0.805	1348	.816	.6168	

[a] Includes estimated 30 mA flow rate for neutralizer.

Table III Summary of thruster performance at various total power

[Accelerator voltage = 300 V;
Discharge voltage = 36 V;
Discharge losses = 198 eV/ion]

Total power, P_T, W	Screen voltage, V_I, V	Beam current, J_B, A	Thrust correction, αF_T,	Main flow rate, $\dot{m}_m$, eq. mA	Cathode flow rate, $\dot{m}_c$, eq. mA	Total flow rate, $\dot{m}_o$, eq. mA (a)	Measured utilization efficiency, η_u	Actual specific impulse, I_{sp}, sec	Actual thrust, T, mN	Thrust to power ratio, T/P, mN/kW	Power efficiency, η_p	Total efficiency, η_T
2646	1100	2.00	0.951	2071	74	2175	0.920	2904	128.6	48.61	0.831	0.691
2244	1100	1.69	0.956	1793	87	1910	0.885	2808	109.3	48.69	0.828	0.670
2246	900	2.00	.951	2132	80	2242	.892	2547	116.4	51.80	.801	.646
1576	900	1.39	0.962	1525	91	1646	0.844	2438	81.8	51.90	0.794	0.620
1348	1100	1.00	0.969	1119	108	1257	0.796	2560	65.5	48.61	0.816	0.610
1301	900	1.14	.966	1267	106	1403	.813	2358	67.4	51.78	.789	.598
1298	700	1.39	.962	1583	91	1704	.816	2078	72.1	55.58	.750	.566
651	1100	0.463	0.983	593	134	757	0.612	1997	30.8	47.28	0.782	0.482
646	830	.580	.980	737	133	900	.644	1820	33.4	51.69	.745	.461
656	600	.760	.975	961	115	1106	.687	1642	37.0	56.42	.695	.454

[a] Assumes 30 mA neutralizer flow rate.

Table IV Isolator flange temperatures at various thruster operating conditions

Screen voltage, V	Beam current, A	Discharge		Cathode isolator flange temp., ^oC	Main isolator flange temp., ^oC	Length of run, hrs
		Losses, eV/ion	Power			
1100	1.0	198	198	197	207	16
1100	.47	250	118	166	183	16
605	.76	198	150	184	197	63

Table V Summary of electrical operating parameters for throttling

Set point	P_T, W	V_I, V	J_B, A	V_A, V	J_A, mA (a)	ΔV_I, V	J_I, A	ϵ_I, eV/ion	J_{mB}, A	J_{CK}, A	V_{CK}, V (a)	T_{mV}, °C (a)	T_{cV}, °C (a)
(a) Profile 1													
15	2650	1100	2	516	4.10	36±0.1	13.00	198	2.40	1.0	5.03	300	289
14	2520	1100	1.9	516	3.86		12.35		2.40		5.12	298	289
13	2390	1100	1.8	516	3.57		11.70		2.40		5.30	295	289
12	2260	1100	1.7	516	3.10		11.05		2.45		5.44	294	289
11	2130	1100	1.6	516	2.91		10.40		2.50		5.65	292	290
10	2000	1100	1.5	516	2.68		9.75		2.55		5.83	289	290
9	1870	1100	1.4	516	2.48		9.10		2.60		6.23	286	294
8	1740	1100	1.3	516	2.36		8.45		2.70		6.45	282	296
7	1610	1100	1.2	516	2.21		7.8		2.75		6.73	280	297
6	1480	1100	1.1	516	2.02		7.15		2.90		7.05	276	299
5	1350	1100	1.0	516	1.90		6.50		3.05		7.46	273	301
4	1220	1100	.9	516	1.78		5.85		3.25		7.85	269	306
3	1038	1100	.76	516	1.59		4.94		3.45		8.65	260	310
2	856	1100	.62	516	1.44		4.03		3.45		9.34	253	312
1	661	1100	.47	516	1.27		3.06		3.05		10.22	245	315
(b) Profile 2													
15	2650	1100	2.0	515	4.10	36±0.1	13.00	198	2.40	1.0	5.03	300	289
14	2520	1100	1.9		3.86		12.35		2.40		5.12	298	288
13	2390	1100	1.8		3.57		11.70		2.40		5.30	296	289
12	2260	1100	1.7		3.10		11.05		2.45		5.44	294	289
11	2130	1100	1.6		2.91		10.40		2.50		5.65	292	290
10	2000	1100	1.5		2.68		9.75		2.55		5.83	289	290
9	1870	1100	1.4		2.48		9.10		2.60		6.23	286	294
8	1740	1100	1.3		2.36		8.45		2.70		6.45	282	296
7	1610	1100	1.2		2.21		7.80		2.75		6.73	280	297
6	1480	1100	1.1		2.02		7.15		2.90		7.05	276	299
5	1350	1100	1.0		1.90		6.50		3.05		7.46	273	301
4	1220	1100	.9	515	1.78		5.85		3.25		7.85	269	306
3	1019	940	.85	445	1.65		5.53		3.35		7.87	267	306
2	822	765	.80	364	1.69		5.20		3.45		8.12	266	306
1	658	605	.76	290	1.80		4.95		3.52		8.33	260	307
(c) Profile 3													
15	2650	1100	2.0	515	3.50	36±0.1	13.00	198	2.40	1.0	5.19	299	295
14	2490	1084	1.9	512	3.27		12.35		2.45		5.29	297	294
13	2329	1066	1.8	507	3.15		11.70		2.50		5.43	296	293
12	2168	1046	1.7	498	2.96		11.05		2.55		5.57	294	292
11	2008	1024	1.6	488	2.83		10.40		2.65		5.76	291	294
10	1847	998	1.5	475	2.65		9.75		2.70		5.93	289	294
9	1688	970	1.4	462	2.54		9.10		2.75		6.16	287	294
8	1526	936	1.3	446	2.33		8.45		2.85		6.38	284	295
7	1366	897	1.2	427	2.23		7.80		3.00		6.67	281	298
6	1207	852	1.1	406	2.04		7.15		3.10		6.96	277	298/9
5	1047	797	1.0	380	1.98		6.50		3.25		7.33	274	301
4	950	758	.94	362	1.91		6.10		3.35		7.56	272	303
3	853	713	.88	340	1.87		5.72		3.45		7.80	270	304
2	758	663	.82	318	1.87		5.33		3.50		8.08	269	305
1	661	605	.76	291	1.81		4.95		3.52		8.36	267	307
(d) Profile 4													
15	2650	1100	2.0	512	3.98	36±0.1	13.00	198	2.40	1.0	5.42	304	319
14	2416	1045	1.9	497	4.04		12.35		2.45		5.57	302	319
13	2192	991	1.8	472	3.88		11.70		2.51		5.75	300	319
12	1988	940	1.7	448	3.79		11.05		2.55		5.93	298	319
11	1802	895	1.6	427	3.67		10.40		2.65		6.15	295	319
10	1616	844	1.5	403	3.50		9.75		2.70		6.36	294	319
9	1450	800	1.4	383	3.24		9.10		2.75		6.58	290	319
8	1298	760	1.3	363	3.14		8.45		2.86		6.85	288	320
7	1160	725	1.2	346	2.92		7.80		3.00		7.15	285	322
6	1036	696	1.1	334	2.80		7.15		3.10		7.49	282	323
5	915	665	1.0	318	2.63		6.50		3.26		7.83	280	325
4	851	652	.94	311	2.56		6.10		3.34		8.06	278	326
3	786	636	.88	304	2.53		5.72		3.45		8.32	277	328
2	718	615	.82	294	2.37		5.35		3.50		8.54	274	330
1	661	606	.76	290	2.07		4.97		3.52		8.78	270	333

[a]Typical.

Table VI Typical thruster performance parameters for various input powers along 4 throttling profiles tested

Profile	Typical power	V_I	J_B	I_{SP}	T/P	η_T	T
1	2650	1100	2	2904	48.61	0.691	128.6
	2250	1100	1.7	2808	48.69	.670	109.3
	1300	1100	.97	2560	48.61	.610	65.5
	660	1100	.463	1997	47.28	.462	30.8
2	2650	1100	2	2904	48.61	0.691	128.6
	2250	1100	1.7	2808	48.69	.670	109.3
	1300	1100	.97	2560	48.61	.610	65.5
	660	605	.76	1642	56.42	.454	37.0
3	2650	1100	2	2904	48.61	0.691	128.6
	2250	1055	1.75	2780	49.2	.665	110.7
	1300	875	1.16	2320	52.2	.595	67.9
	660	605	.76	1642	56.42	.454	37.0
4	2650	1100	2	2904	48.61	0.691	128.6
	2250	1005	1.83	2690	50.00	.658	112.5
	1300	760	1.30	2170	54.40	.580	70.7
	660	605	.76	1642	56.42	.454	37.0

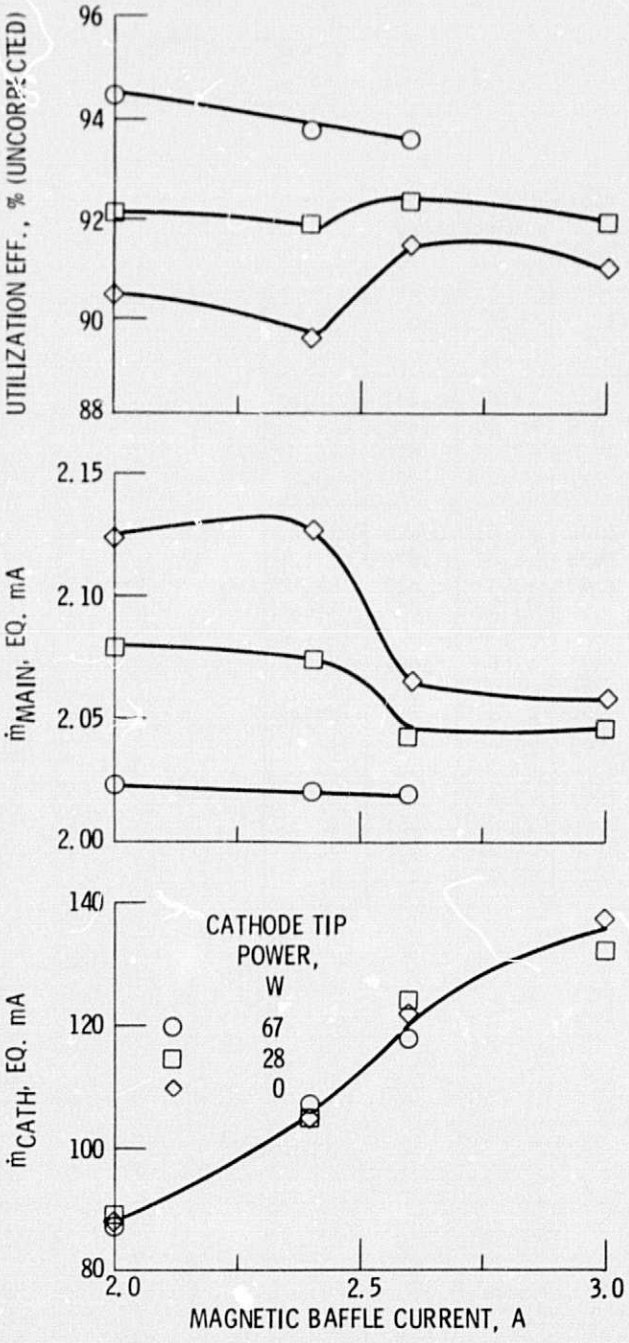

Figure 1. - Effect of tip heater power on thruster SN 804 with a recessed impregnated insert V_I = 1100 V. Beam current, 2.0 A; discharge voltage, 35 V; discharge losses, 185 eV/ion.

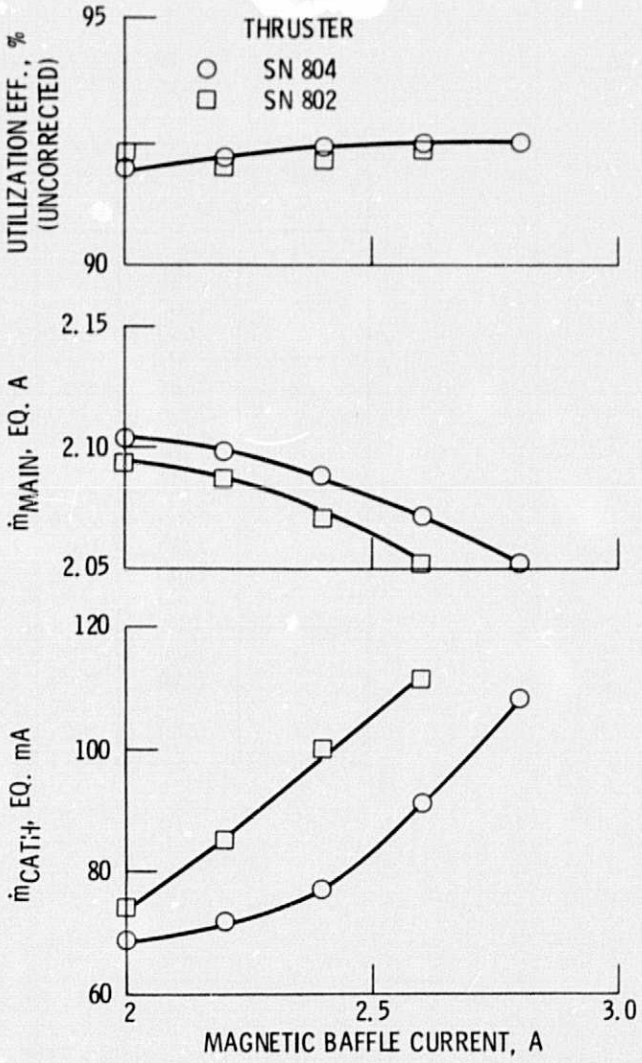

Figure 2. - Comparison performance of two 30-cm EM thrusters at 2 A beam. Discharge voltage = 35 V; discharge losses = 185 eV/ion.

E-8952

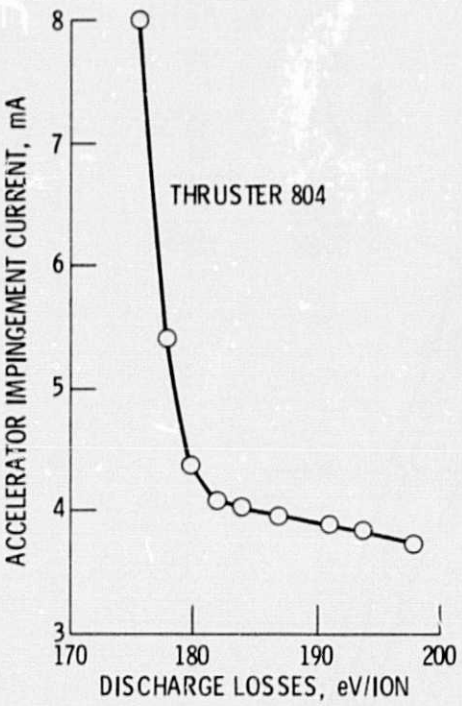

Figure 3. - Variation of accelerator impingement current with discharge losses. Discharge voltage = 36 V; beam current = 2.0 A.

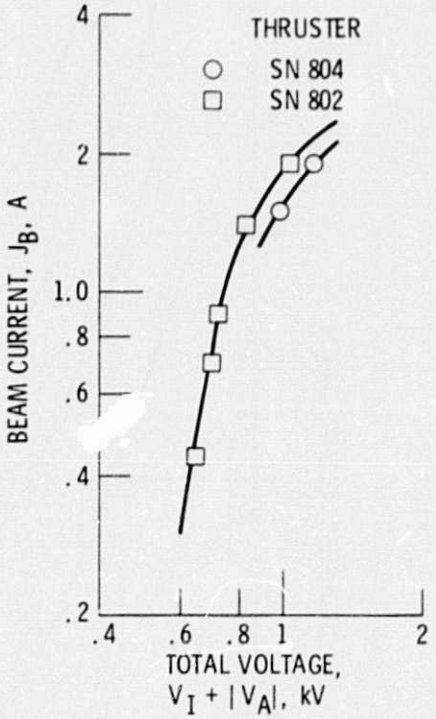

Figure 4. - Beam current capability (perveance) of extraction grids tested.

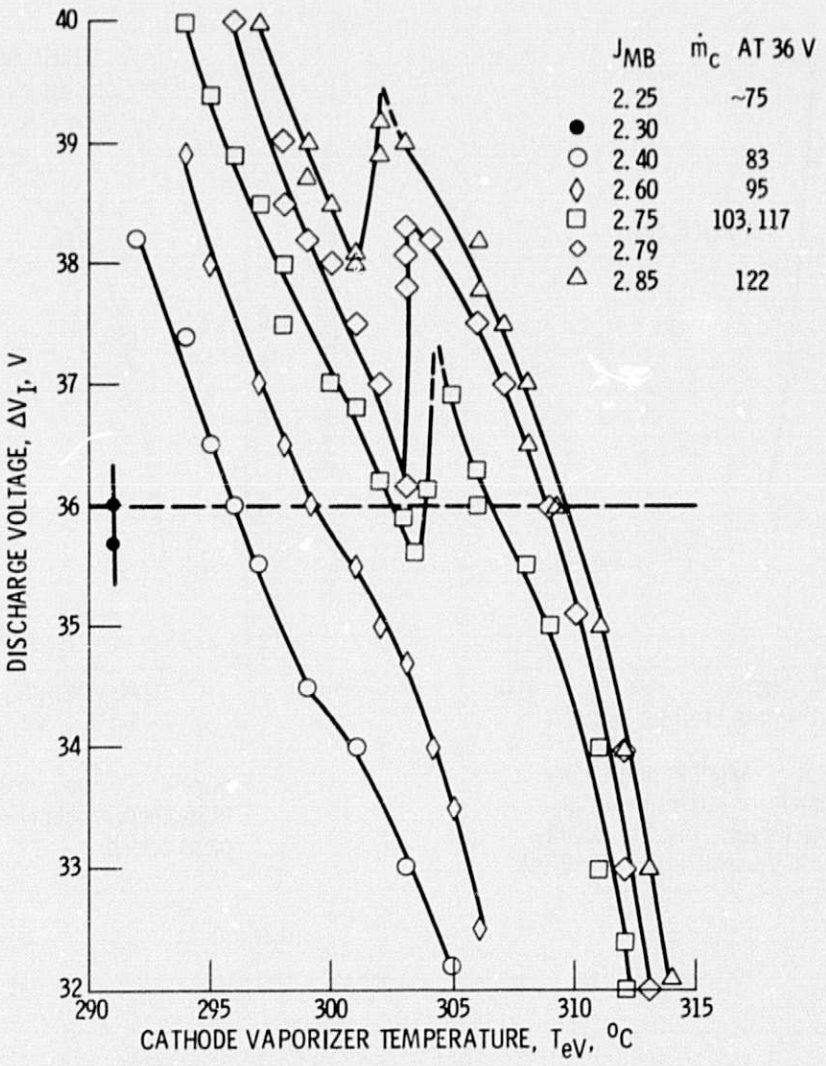

Figure 5. - Discharge voltage as function of cathode vaporizer temperature and flow rate. J_B = 2.0 A; V_I = 1100 V; ε_I = 198 eV/ion.

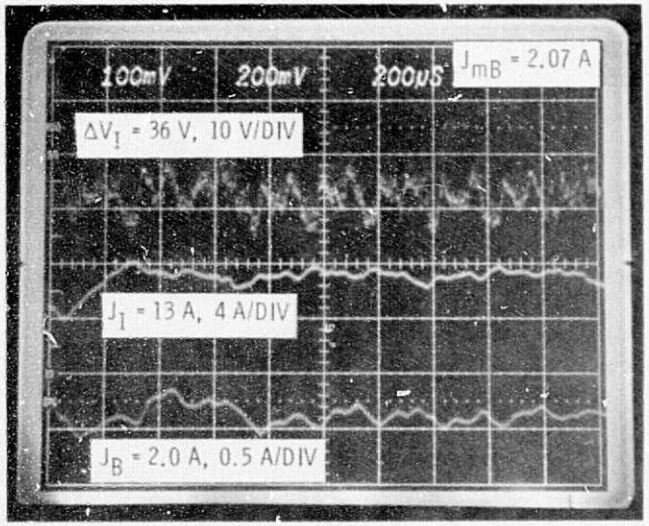

(a) LOW FLOW REGION.

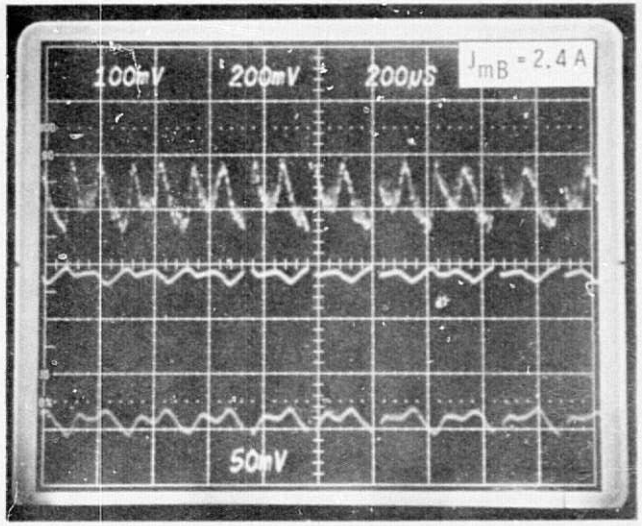

(b) NORMAL OPERATING REGION.

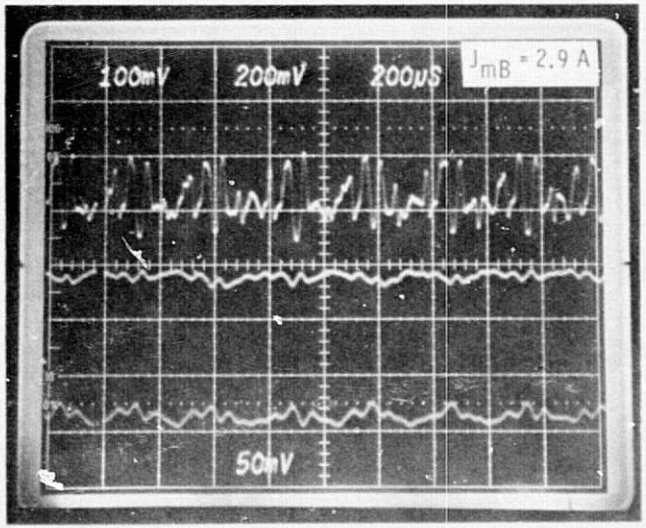

(c) HIGH FLOW REGION.

Figure 6. - Discharge voltage and current at various mag baffle currents.

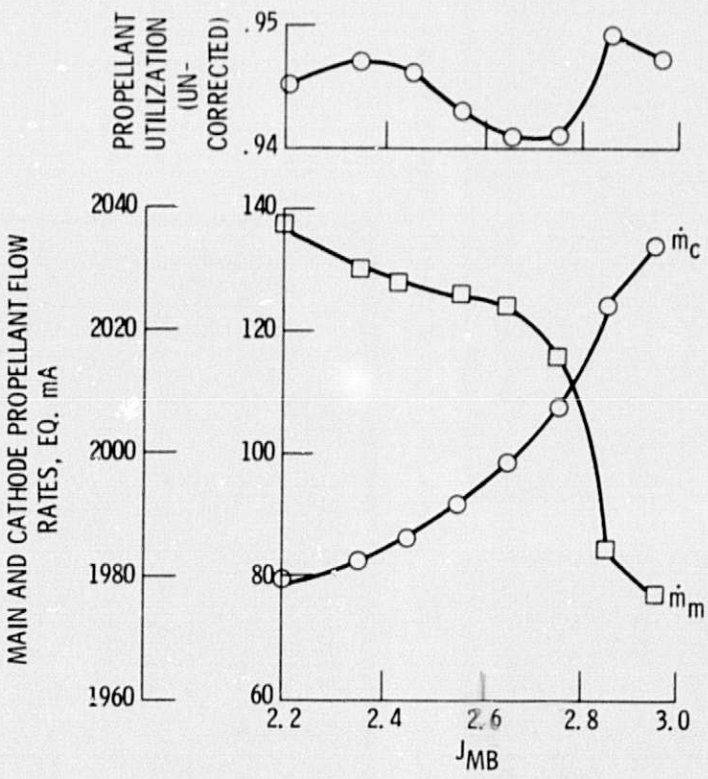

Figure 7. - Thruster performance as function of magnetic baffle current. J_B = 2.0A V_I = 1100 V, ε_I = 198 eV/ion.

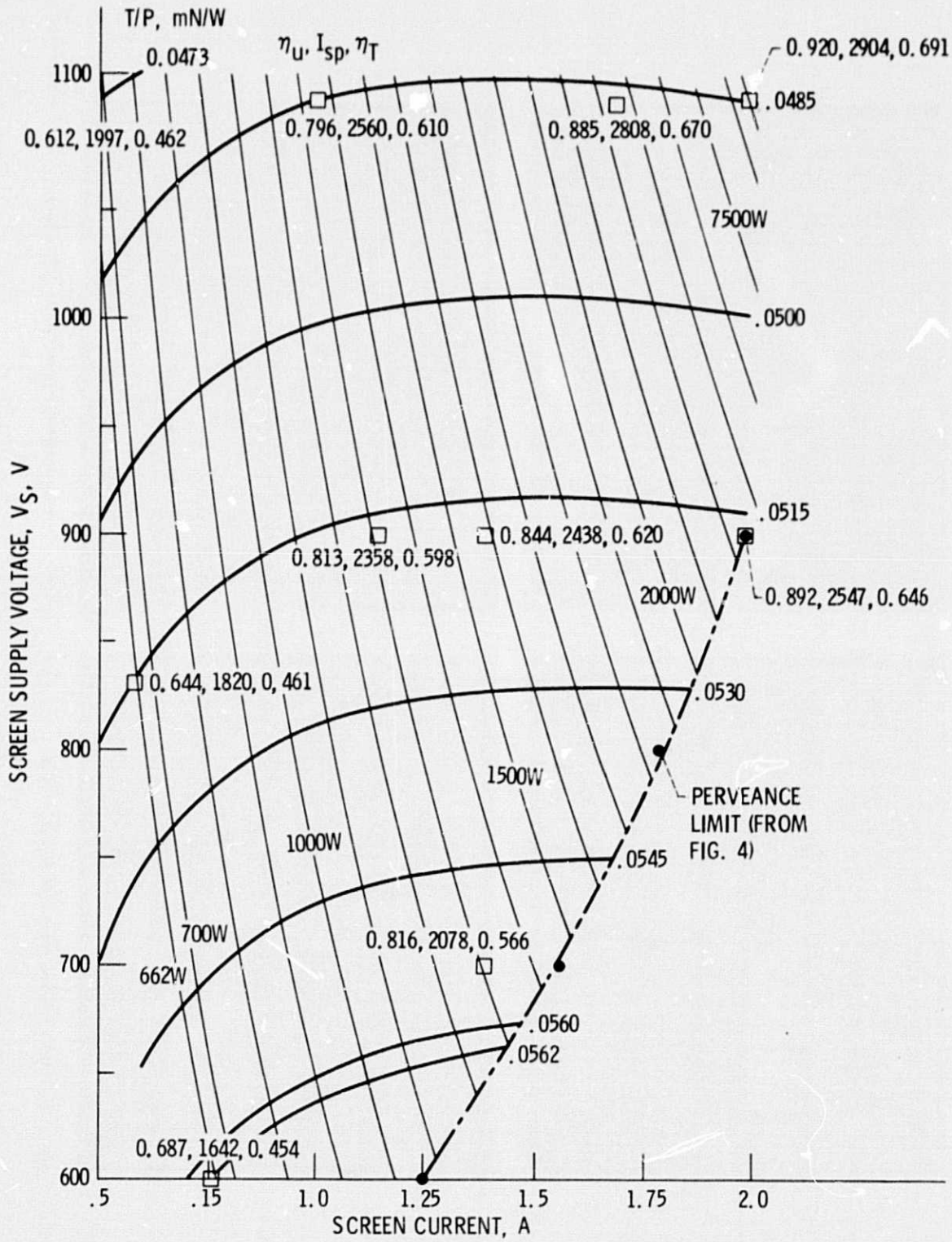

Figure 8. - Constant power and thrust/power for screen voltages and currents within power supply operating envelope. Discharge voltage = 36 V; discharge losses = 198 eV/ion.

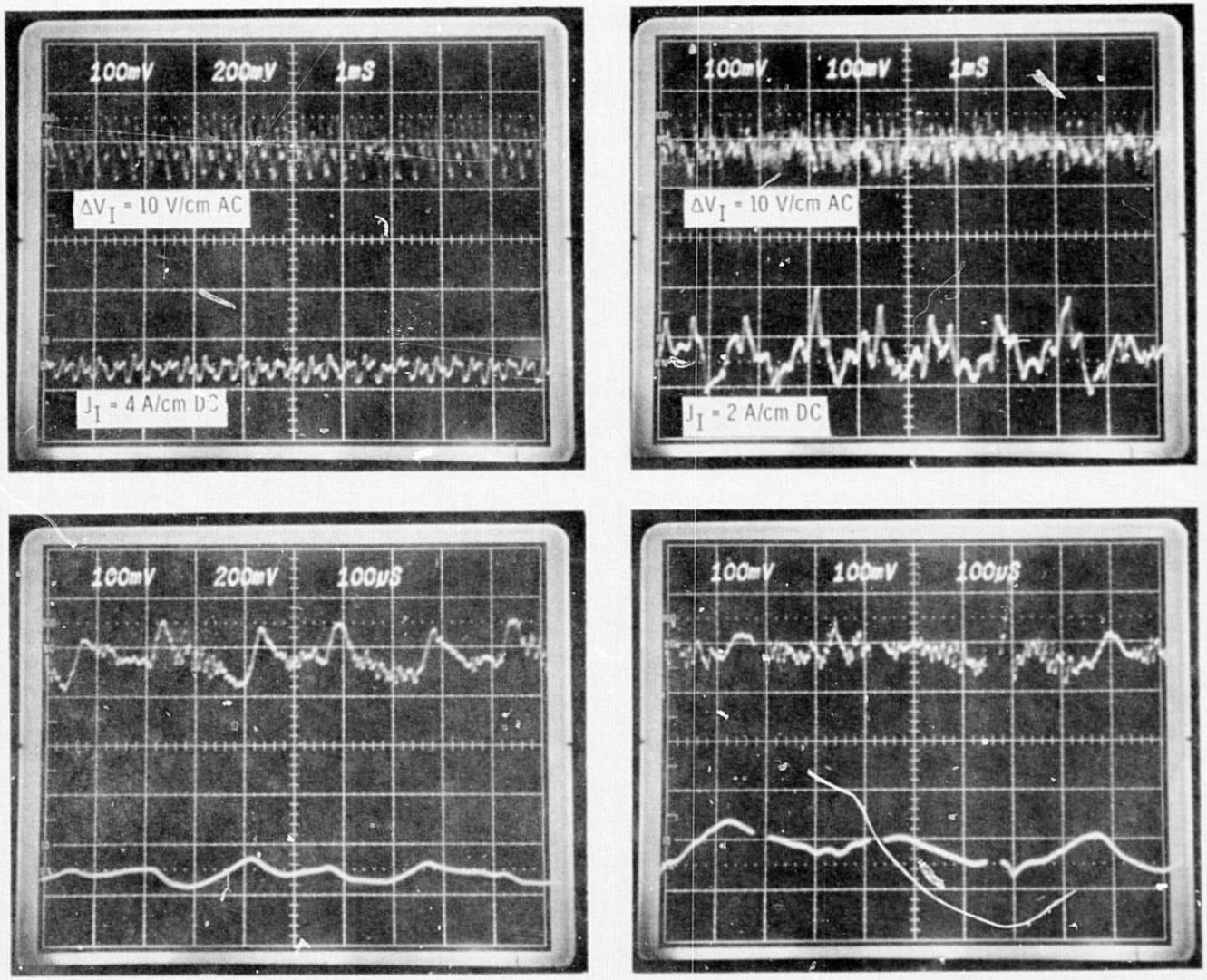

(a) V_I = 605 V, J_B = 0.76 A, ΔV_I = 36 V.

(b) V_I = 1100 V, J_B = 0.47 A, ΔV_I = 36 V.

Figure 9. - Comparison of discharge oscillations at 1/4 power.

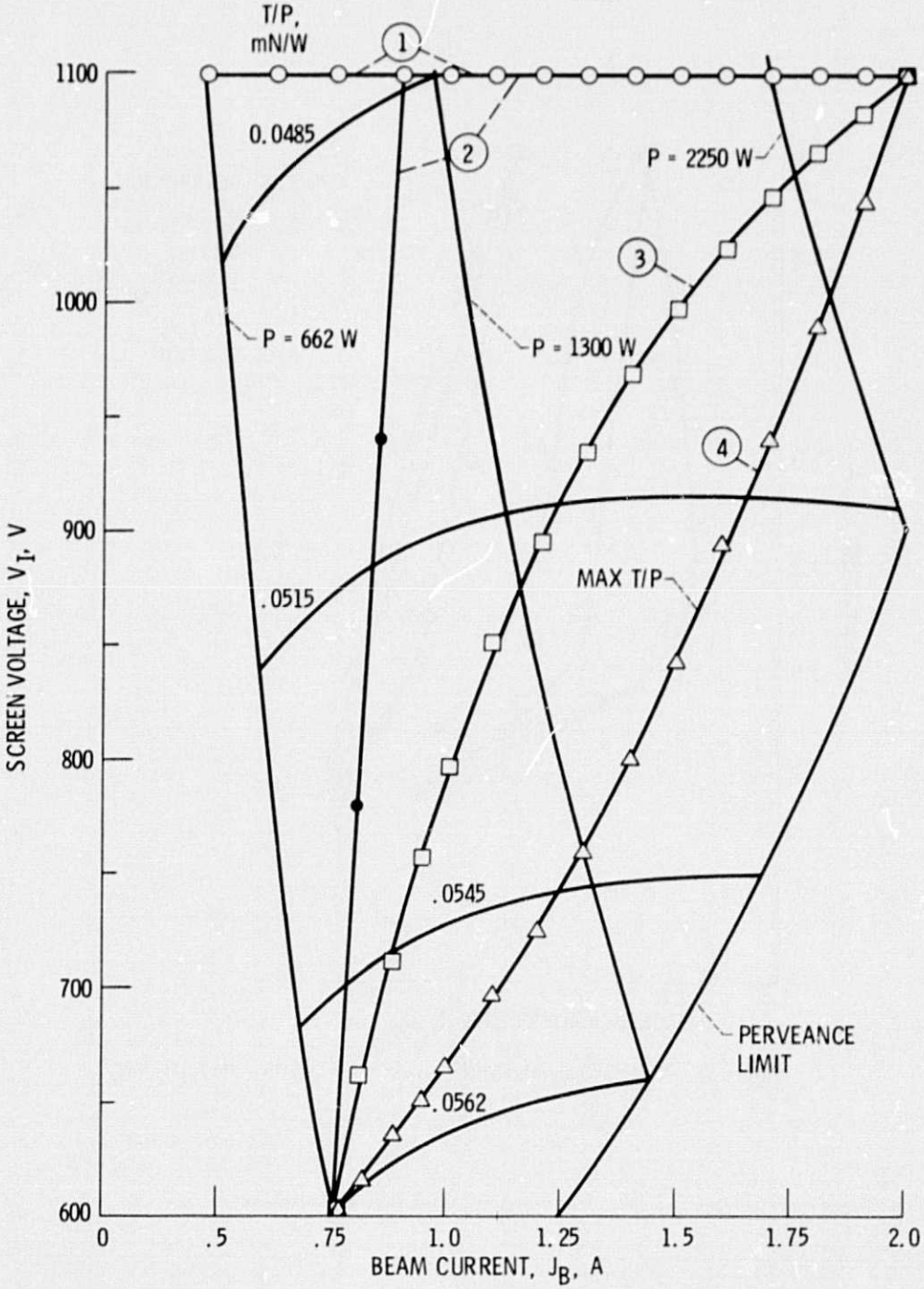

Figure 10. - Four throttling profiles tested shown on parameters of figure 8.

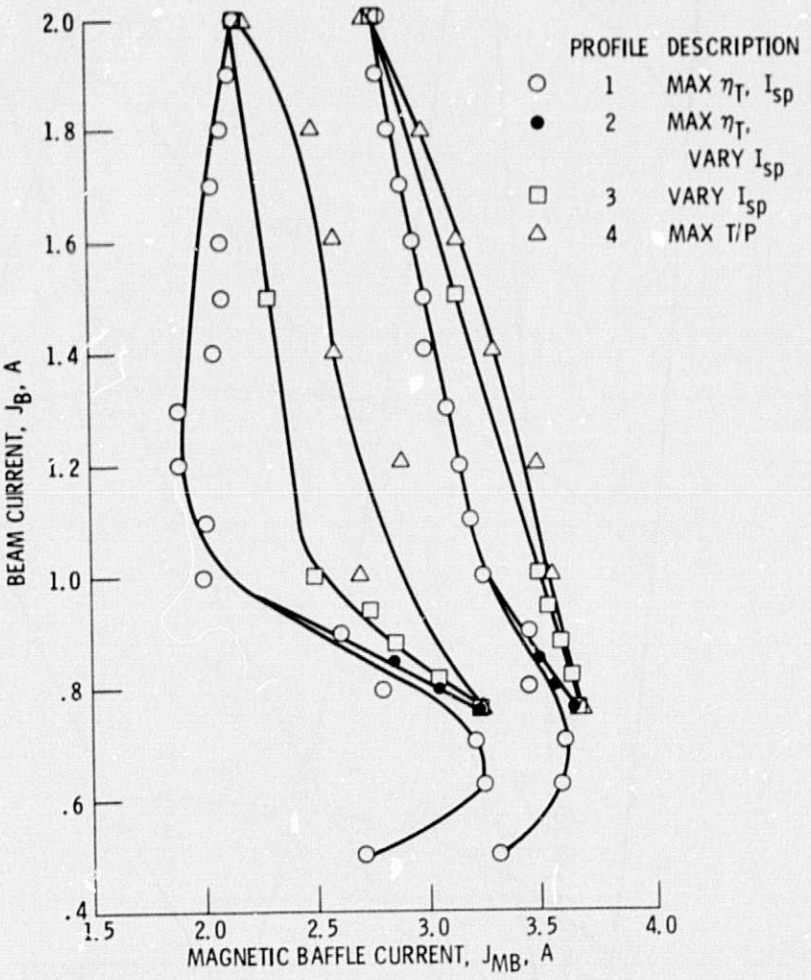

Figure 11. - Critical magnetic baffle currents for four throttling profiles.

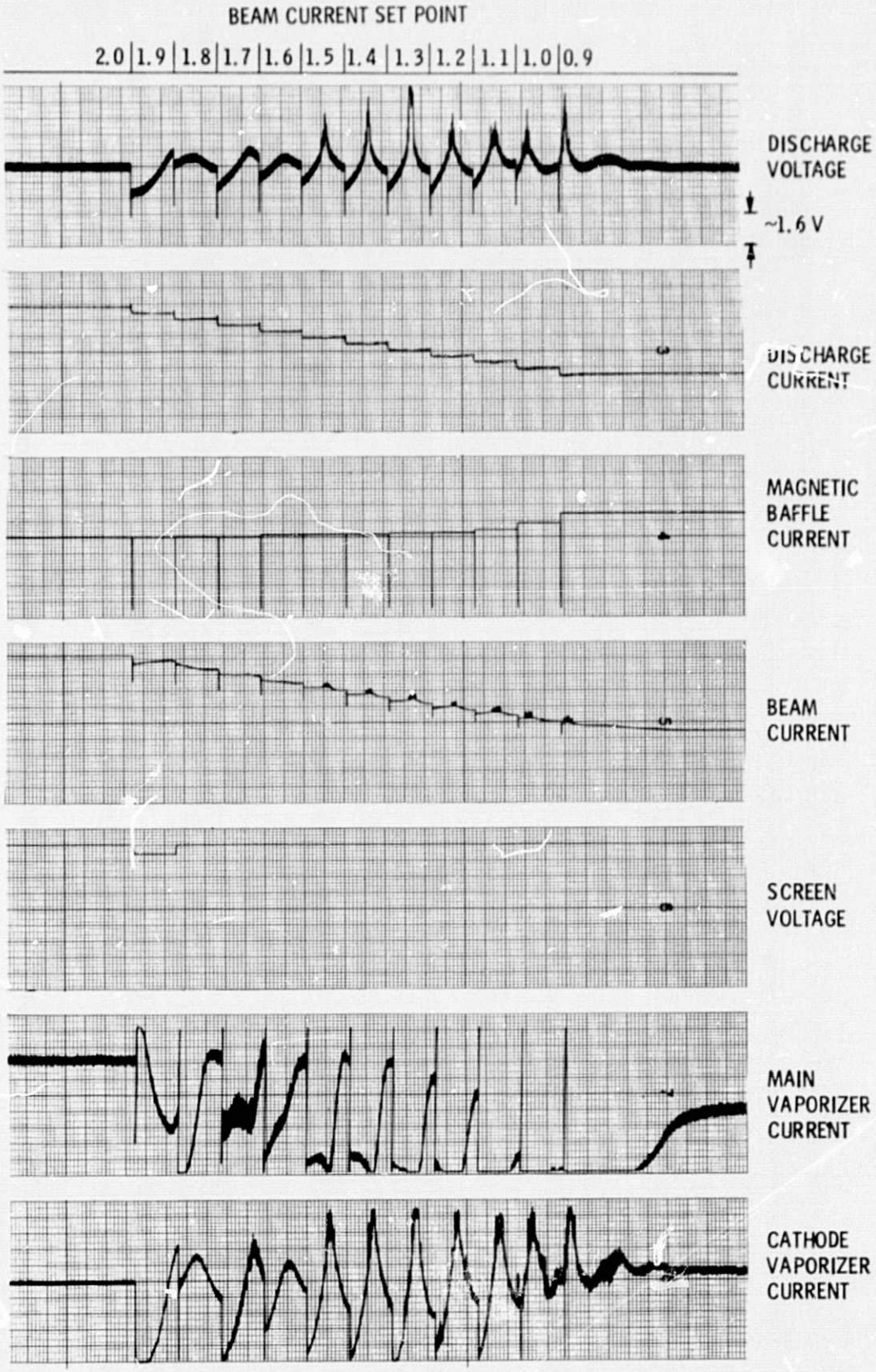

Figure 12. - Throttling performance down from 2.0 to 0.9 A beam current, time increment = 10.7 sec.

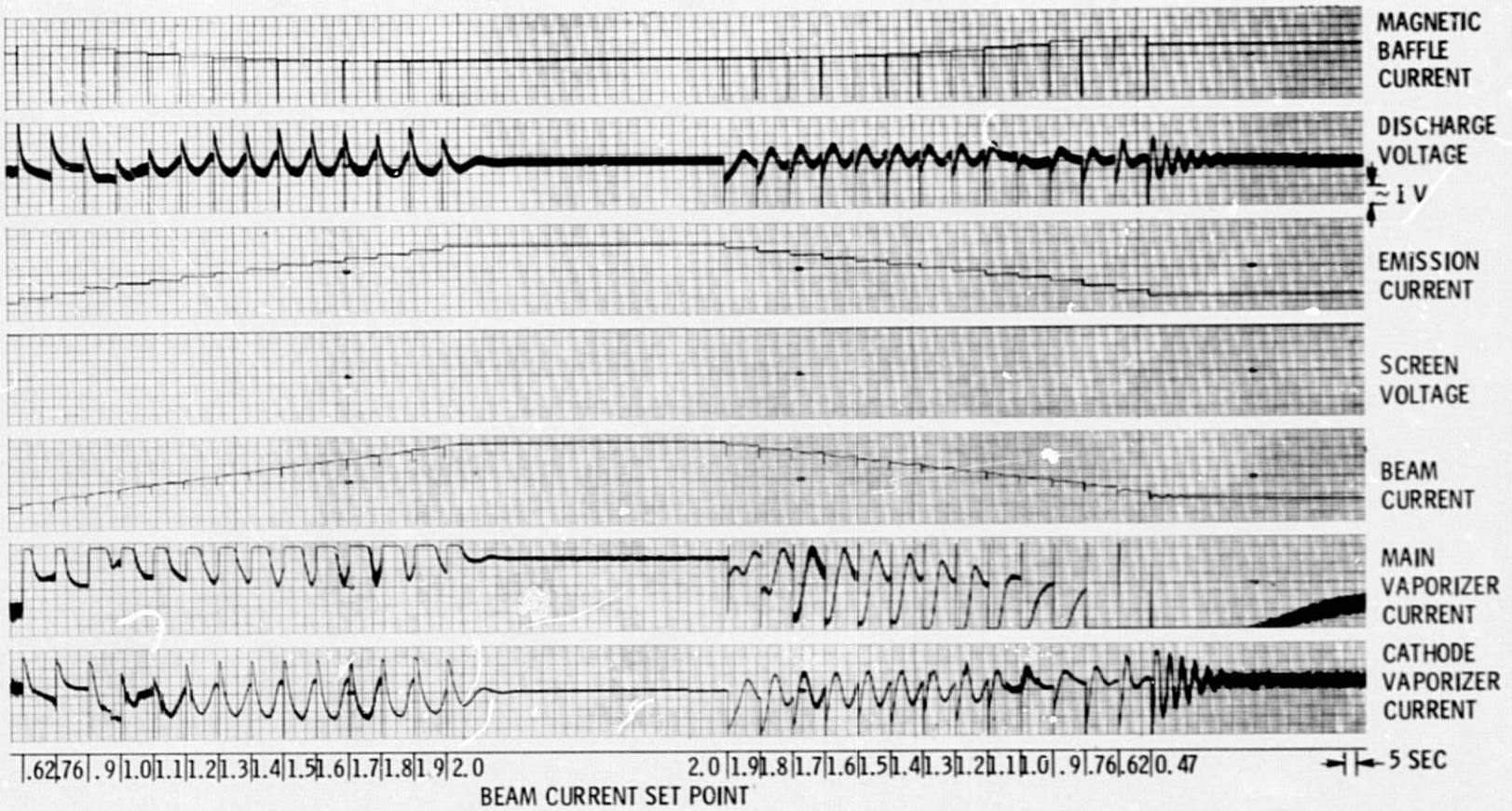

(a) PROFILE 1.

Figure 13. - Dynamic throttling for each of profiles of figure 10 and table V.

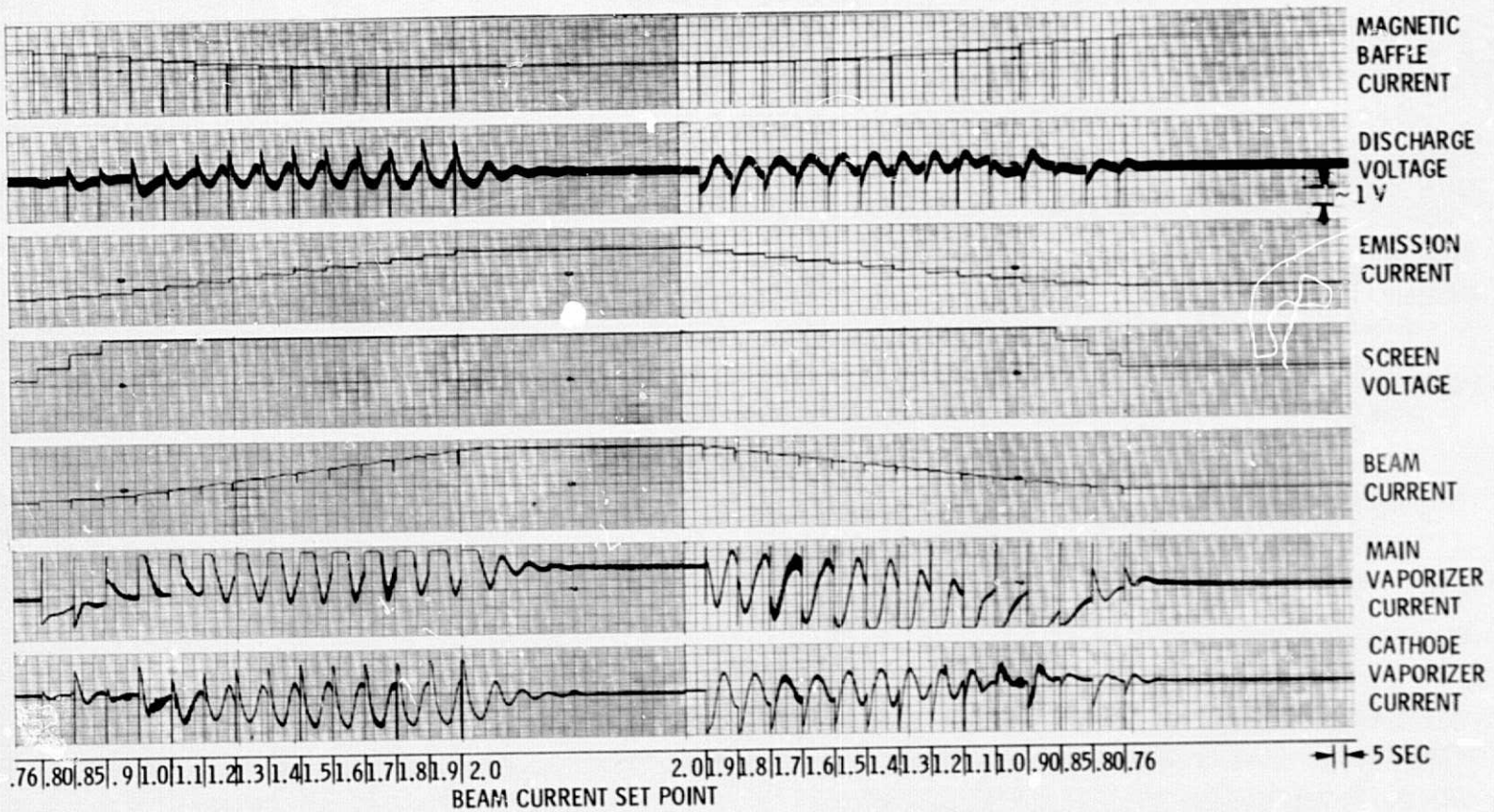

(b) PROFILE 2.

Figure 13. - Continued.

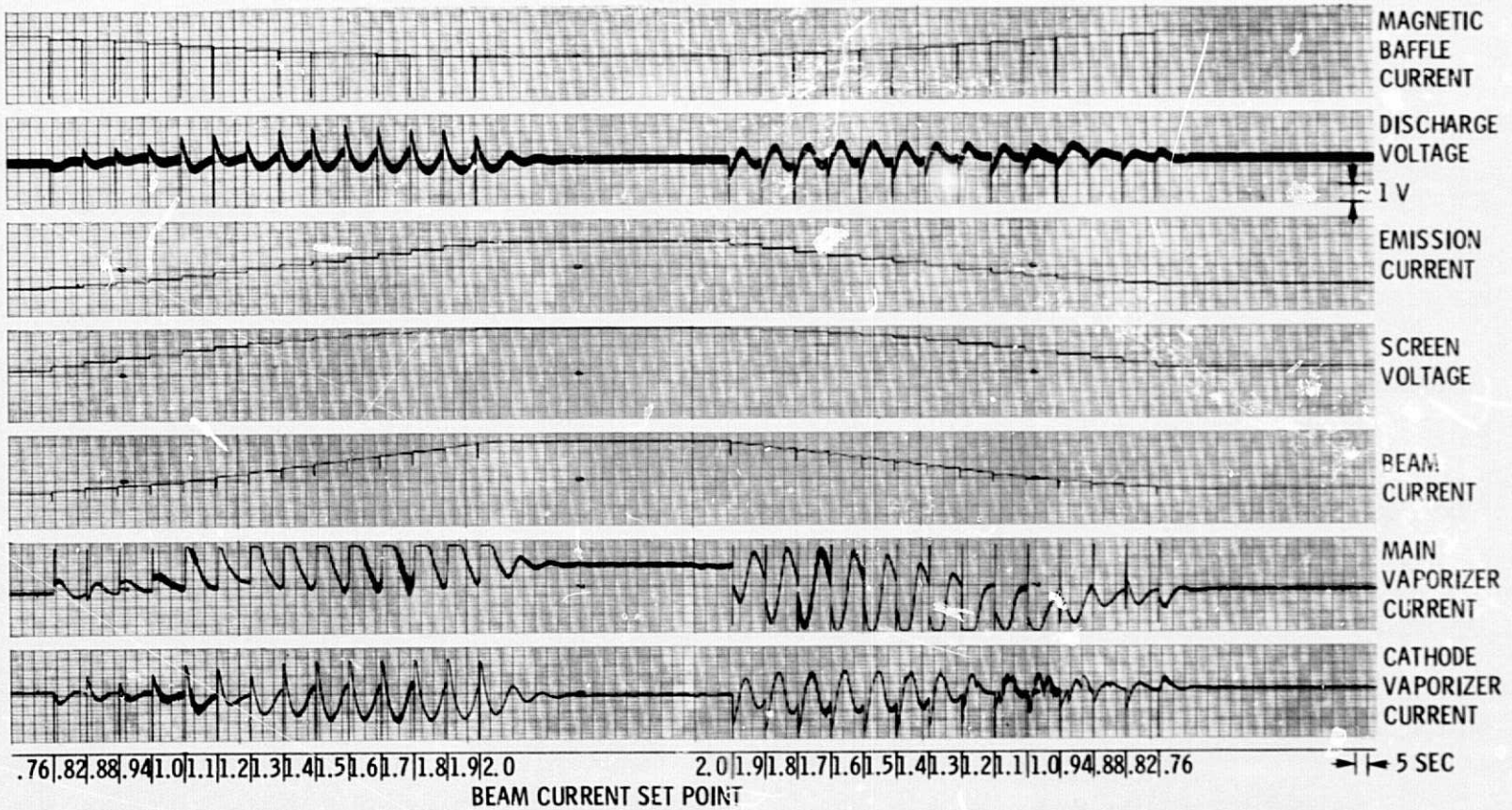

(c) PROFILE 3.

Figure 13. - Continued.

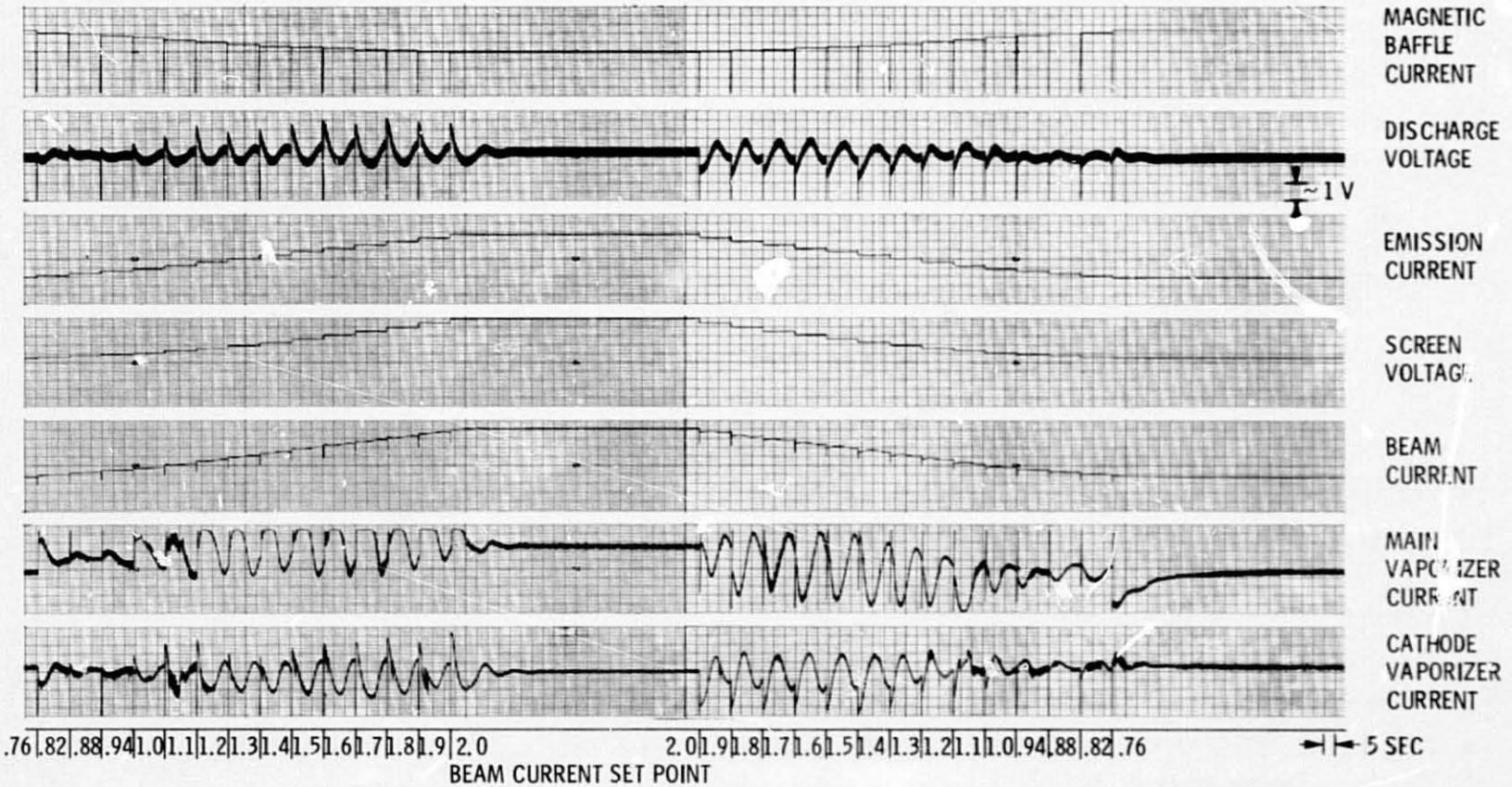

(d) PROFILE 4.

Figure 13. - Concluded.

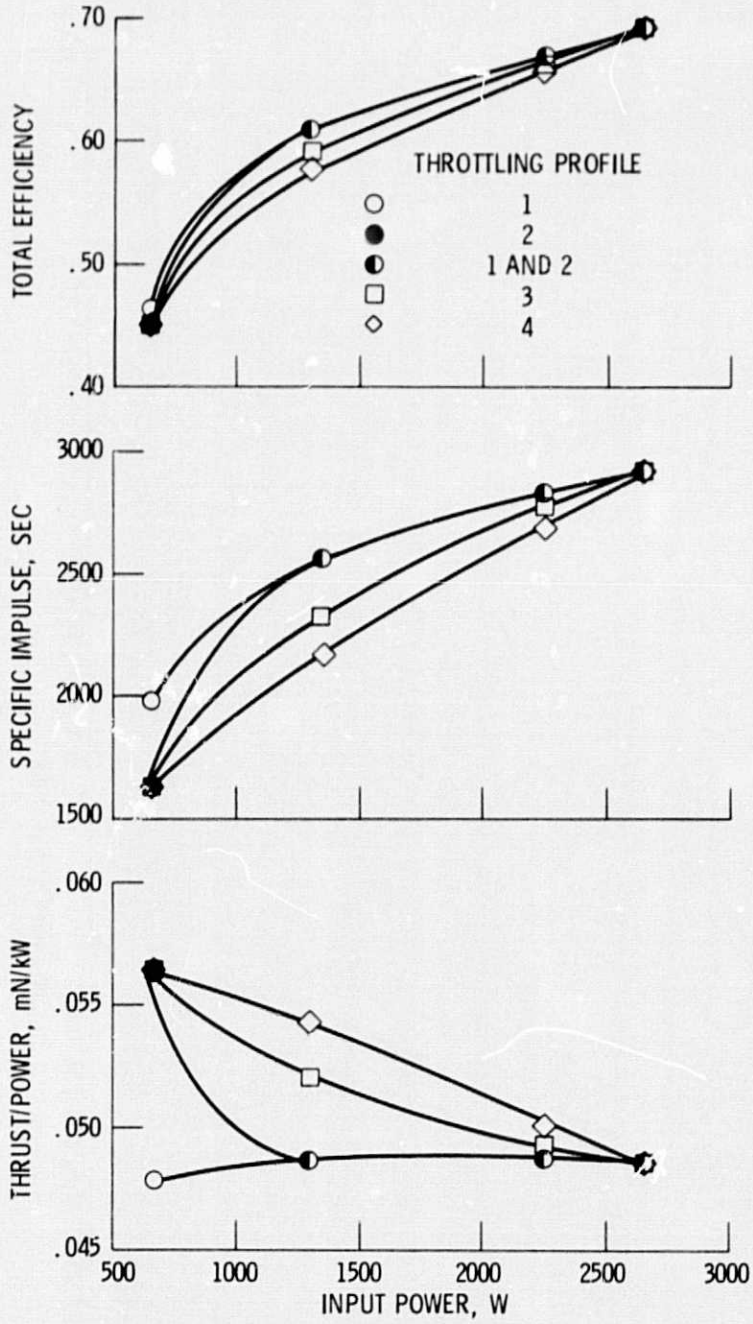

Figure 14. - Thruster performance over input power range for the four profiles tested.

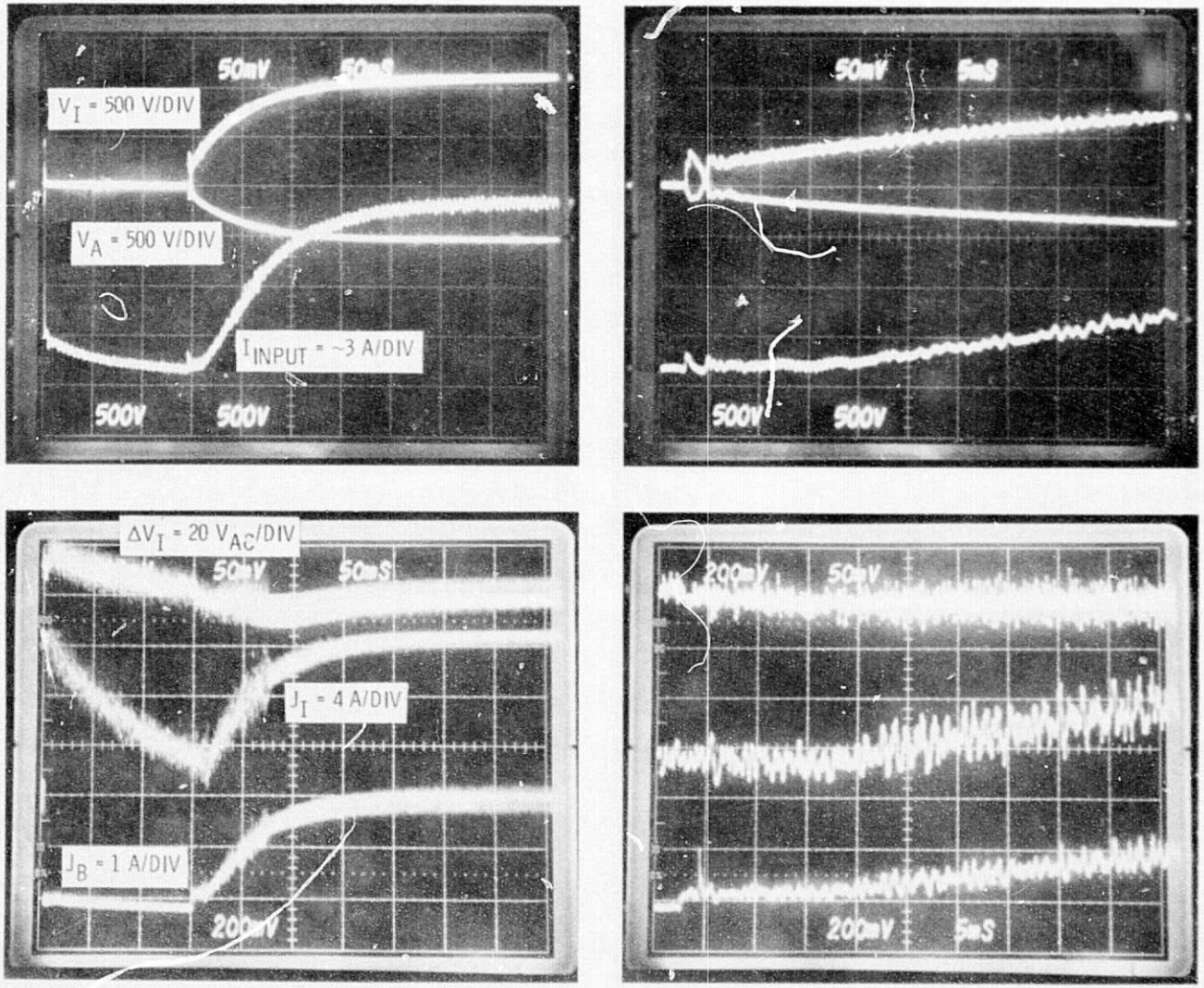

(a) 50 msec/DIV.

(b) 5 msec/DIV - STARTING ~150 msec AFTER START OF RECYCLE SEQUENCE.

Figure 15. - High voltage recycle at beam current = 2 A; screen voltage, 1100 V operating point.

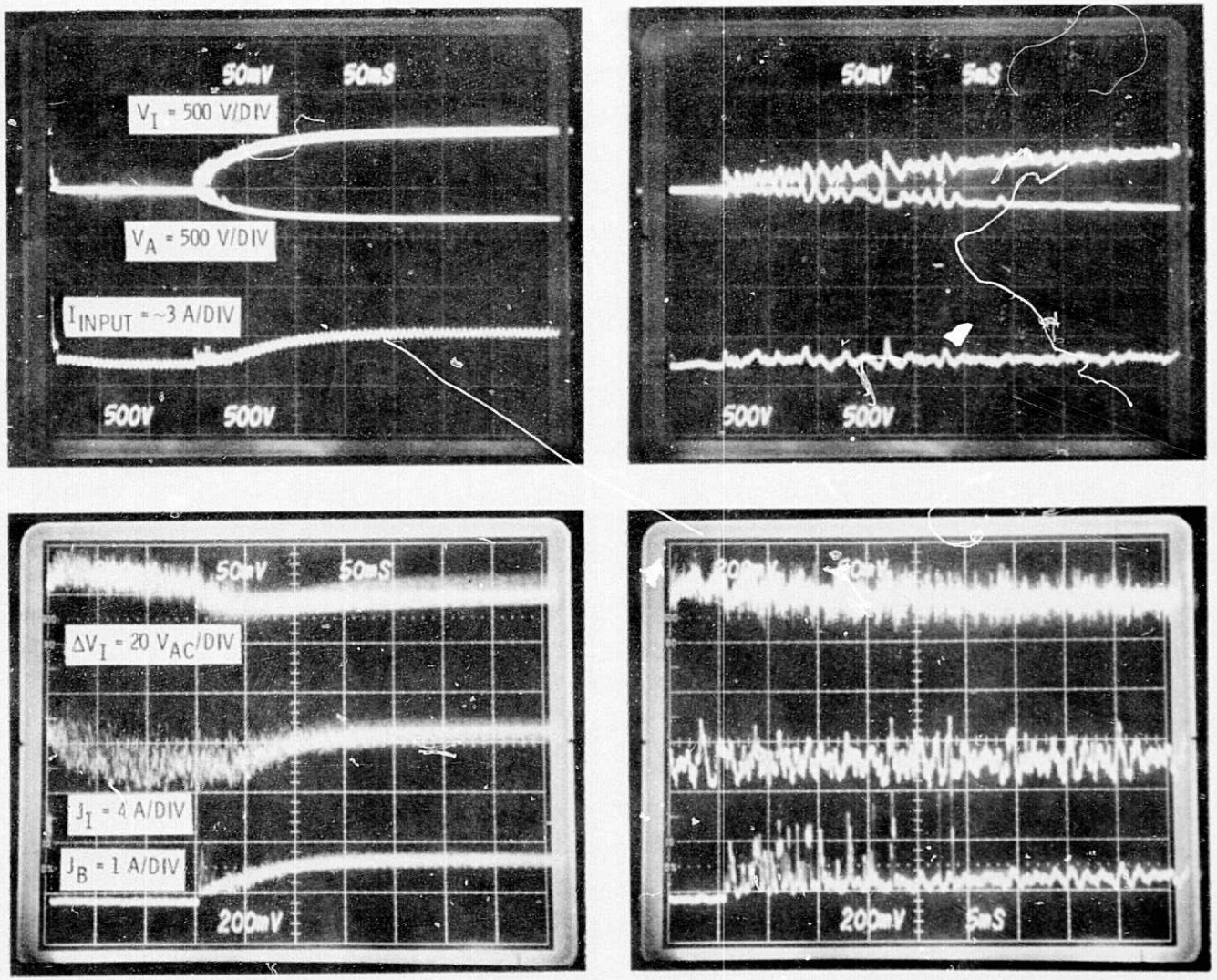

(a) 50 msec/DIV.

(b) 5 msec/DIV - STARTING ~ 150 msec AFTER START OF RECYCLE SEQUENCE.

Figure 16. - High voltage recycle at beam current = .76 A; screen voltage, 600 V operating point.

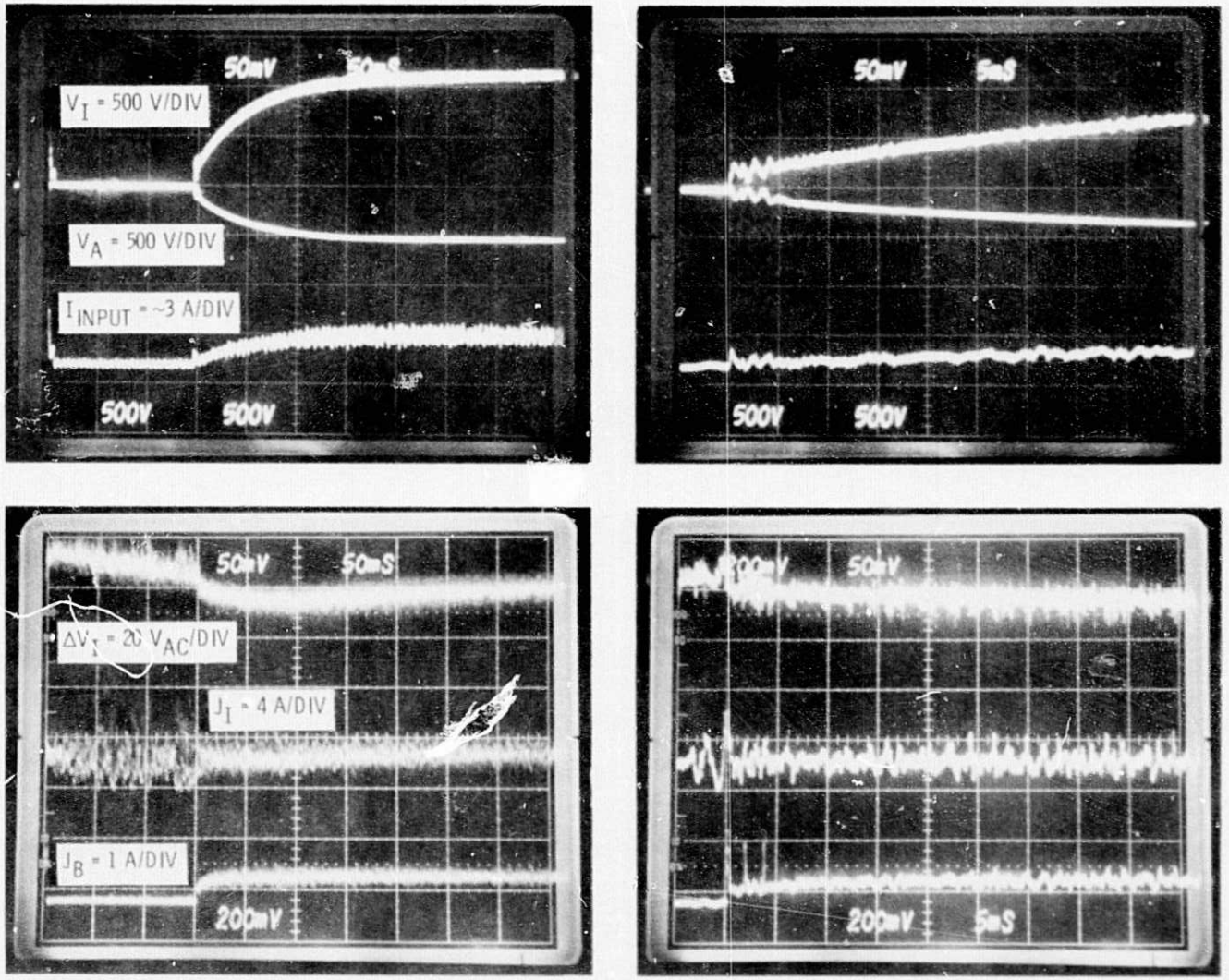

(a) 50 msec/DIV.

(b) 5 msec/DIV - STARTING ~ 150 msec AFTER START OF RECYCLE SEQUENCE

Figure 17. - High voltage recycle at beam current = .47 A; screen voltage, 1100 V operating point.

Table AI Summary of fixed power losses

2.0 A beam			0.5 A beam	
P_{VAPS}		12.4 W		12.0 W
P_{HTRS}		0		0
P_{CK}	5.2 V × 1.0 A	5.2	8.9 V × 1.0 A =	8.9
P_{NK}	15 V × 1.8 A	27.0	16.7 V × 1.8 A =	30 0
P_{mB}	1.3 V × 2.4 A =	3.1	2.0 V × 3.6 A =	7.2
$V_A J_A$	500 V × 4 mA =	2.0	500 V × 1 mA =	0.5
		49.7 W		58.6 W

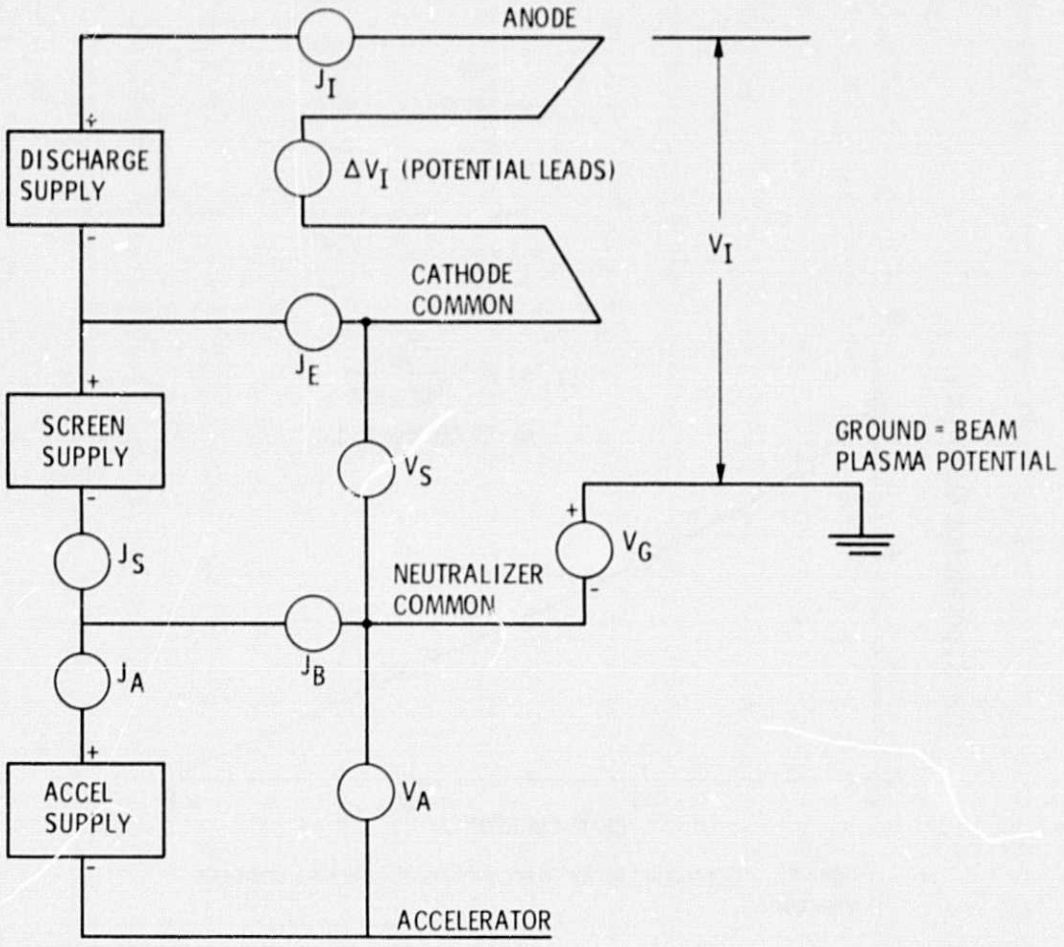

E-8952

V_S	OUTPUT VOLTAGE OF SCREEN SUPPLY, V
J_S	OUTPUT CURRENT OF SCREEN SUPPLY, A
V_I	NET ION ACCELERATING POTENTIAL, V
V_G	NEUTRALIZER TO BEAM COUPLING POTENTIAL, V
J_B	BEAM CURRENT, A
V_A	ACCELERATOR SUPPLY VOLTAGE, V
J_A	ACCELERATOR CURRENT, mA
ΔV_I	DISCHARGE POTENTIAL DIFFERENCE, V
J_E	DISCHARGE EMISSION CURRENT, A
J_I	TOTAL DISCHARGE CURRENT, A

$$J_S = J_B + J_A \approx J_B$$
$$J_I = J_S + J_E$$
$$V_I = V_S + \Delta V_I - |V_G| \approx V_S$$

Figure A1. - Instrumentation schematic and symbol definition.

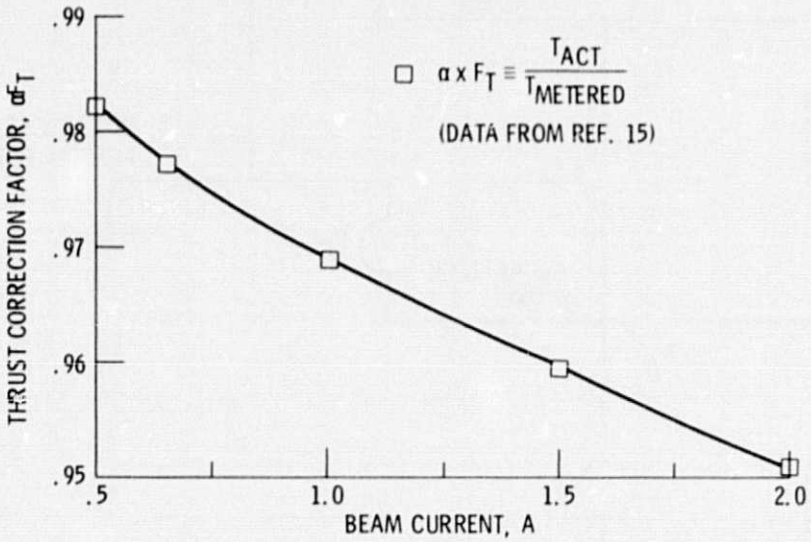

Figure A2. - Correction factor to account for double ions and beam divergence.

NASA-Lewis